Dark Matter Clumps and Streams
From Numerical Simulations to Detection Efforts

Michael Kuhlen, UC Berkeley

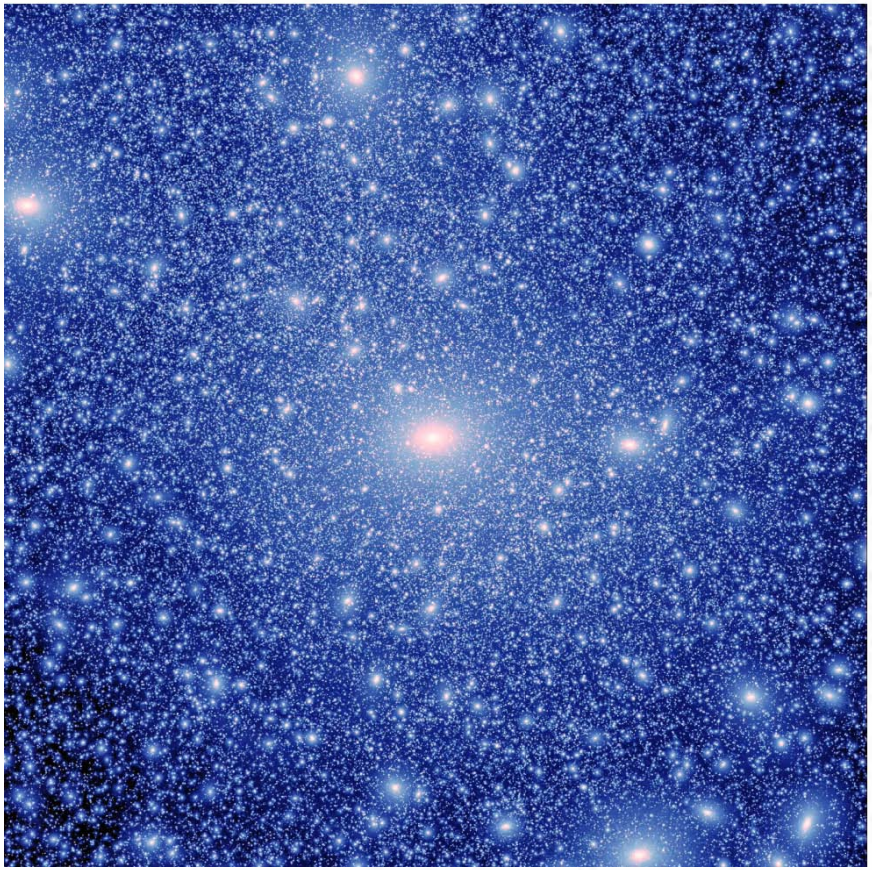

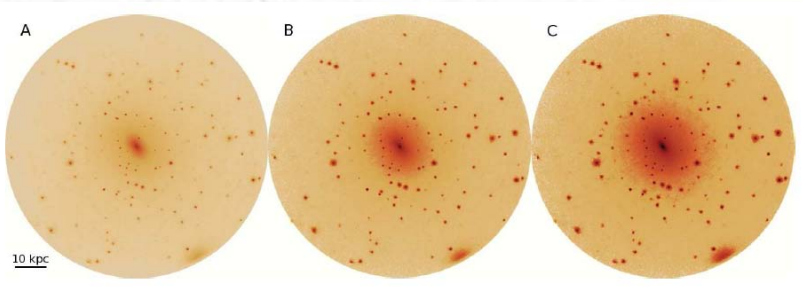

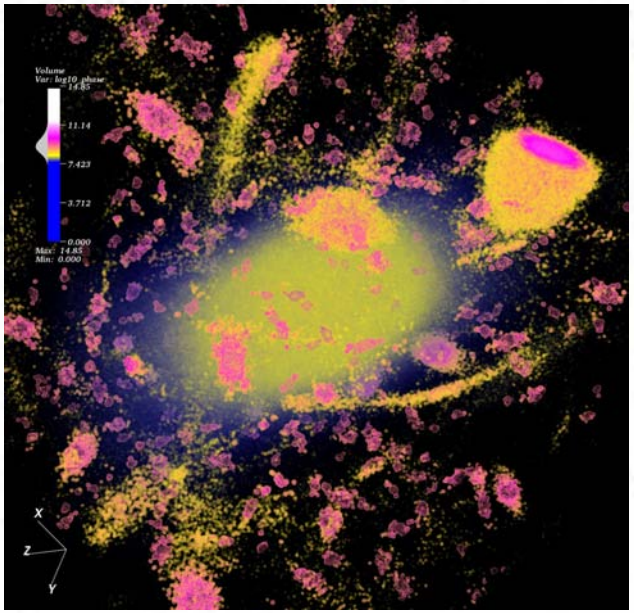

The Via Lactea collaboration

(P. Madau, J. Diemand, M. Zemp, B. Moore, J. Stadel, D. Potter, V. Rashkov)

Dark Matter Clumps and Streams
From Numerical Simulations to Detection Efforts

Michael Kuhlen, UC Berkeley

Outline

- Numerical Simulations State-of-the-Art
- Substructure: Astrophysics
- Substructure: Particle physics
  - As individual sources of DM annihilation: dwarf galaxies and dark subhalos
  - As a diffuse background from the cumulative annihilation in all Galactic subhalos
  - As an annihilation “boost factor”
  - As signatures in direct detection experiments
- Conclusions

I. Dark Matter Simulations: The State Of The Art

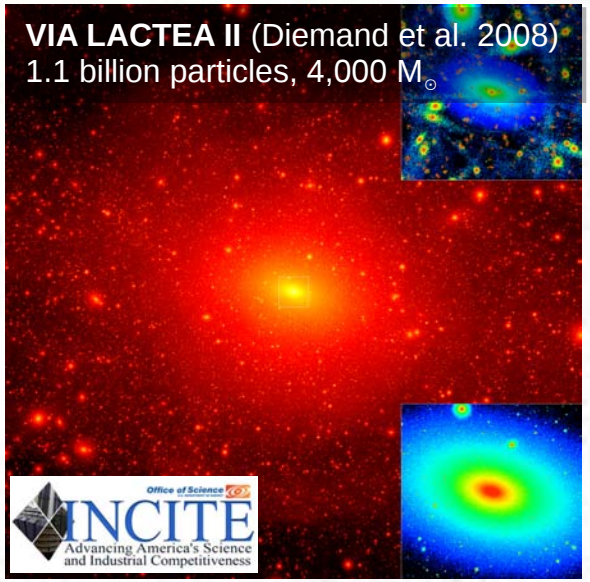

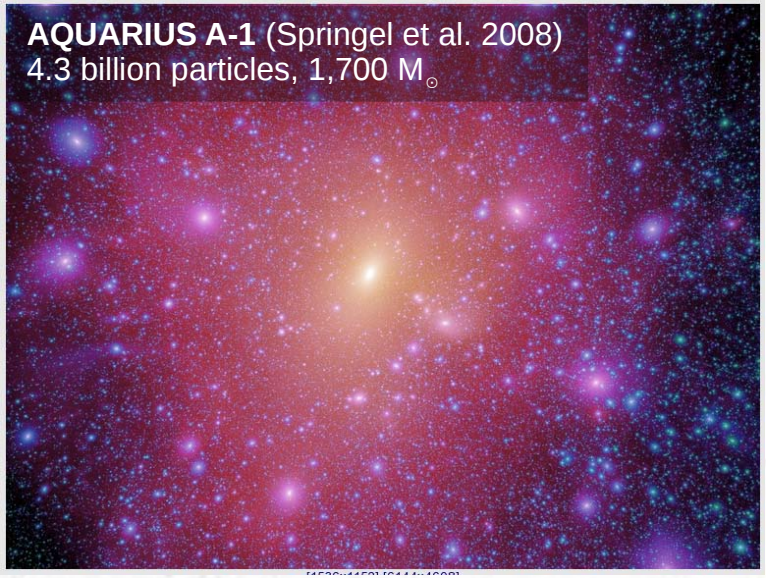

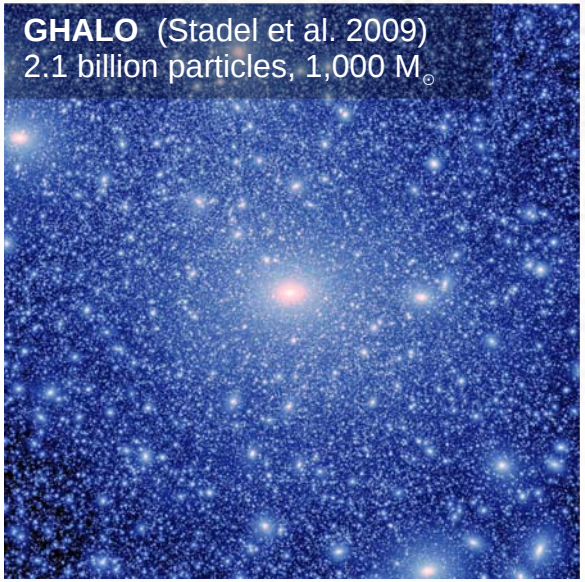

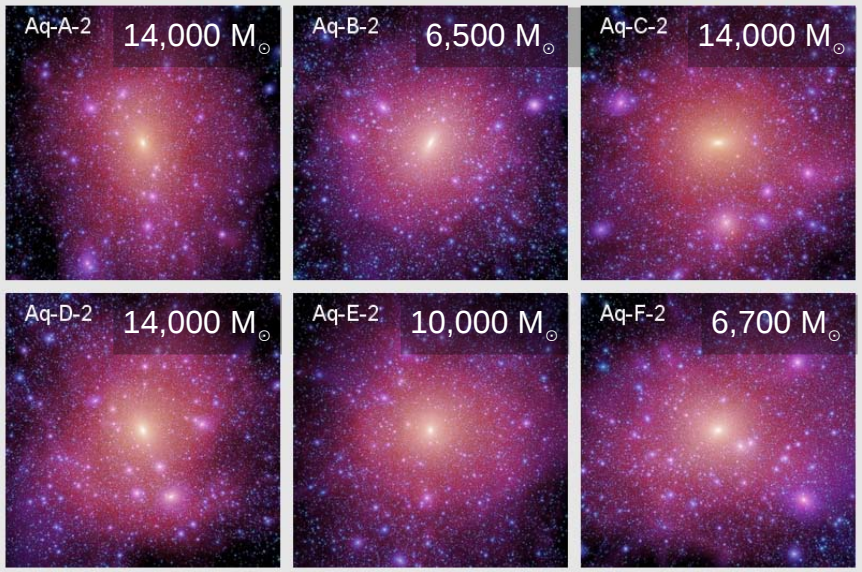

Via Lactea II/GHALO vs. Aquarius

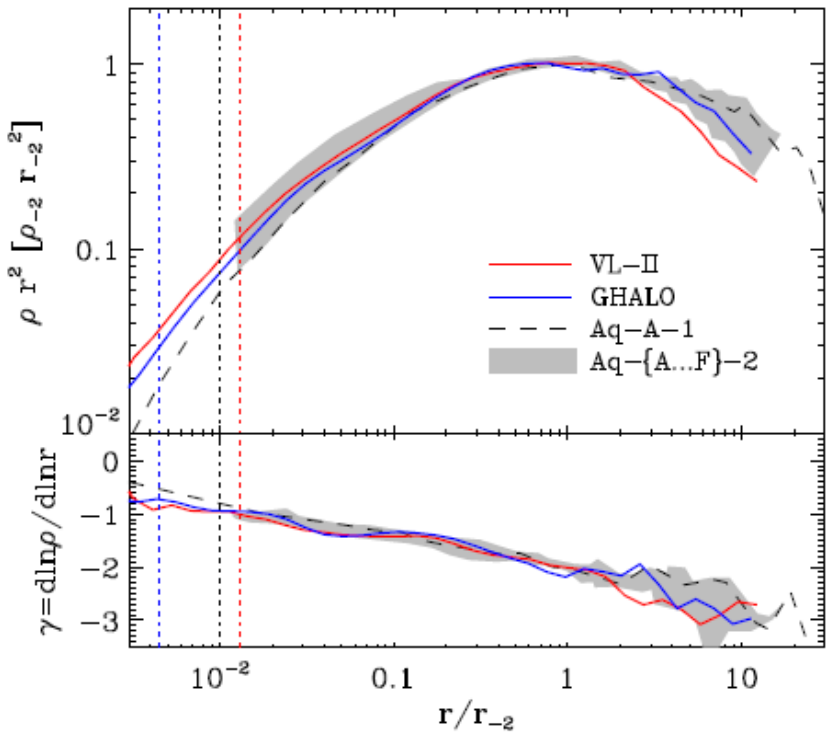

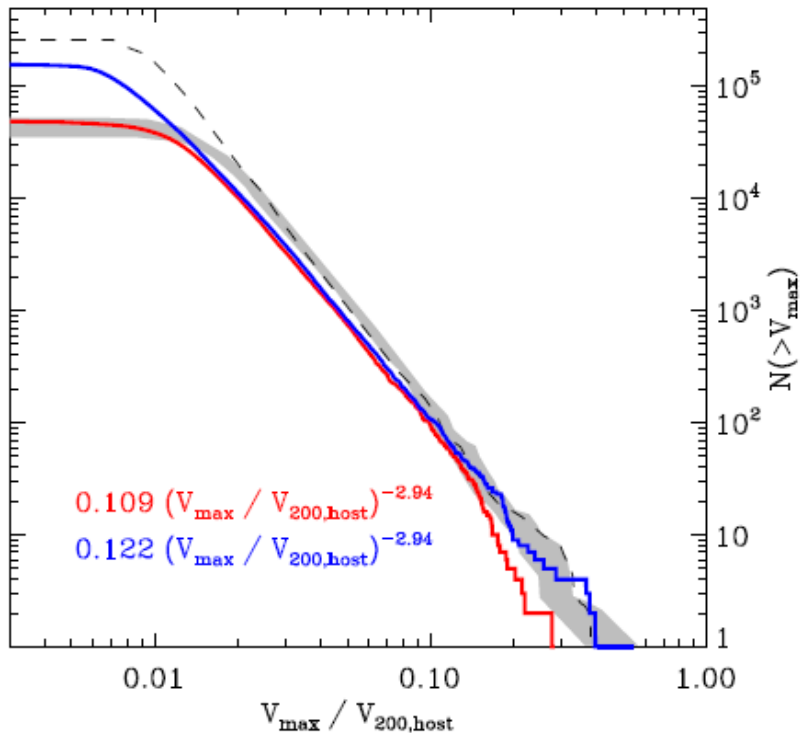

Via Lactea II, GHALO: **PKDGRAV2m**
Aquarius: **Gadget-3**

Once appropriately scaled, VL-II, GHALO, and Aquarius agree with each other.

Via Lactea II/GHALO vs. Aquarius

Comparison with Bolshoi simulation

2048^3 particles in 250 h^{-1} Mpc box
$m_p = 1.35 \times 10^8\ h^{-1}\ M_\odot$
10 million halos and subhalos

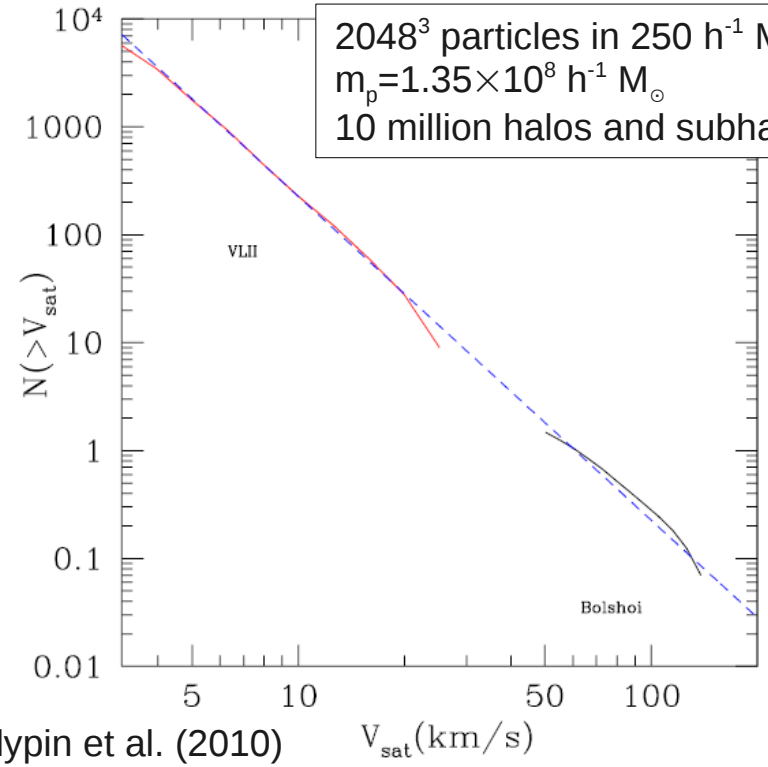

Klypin et al. (2010)

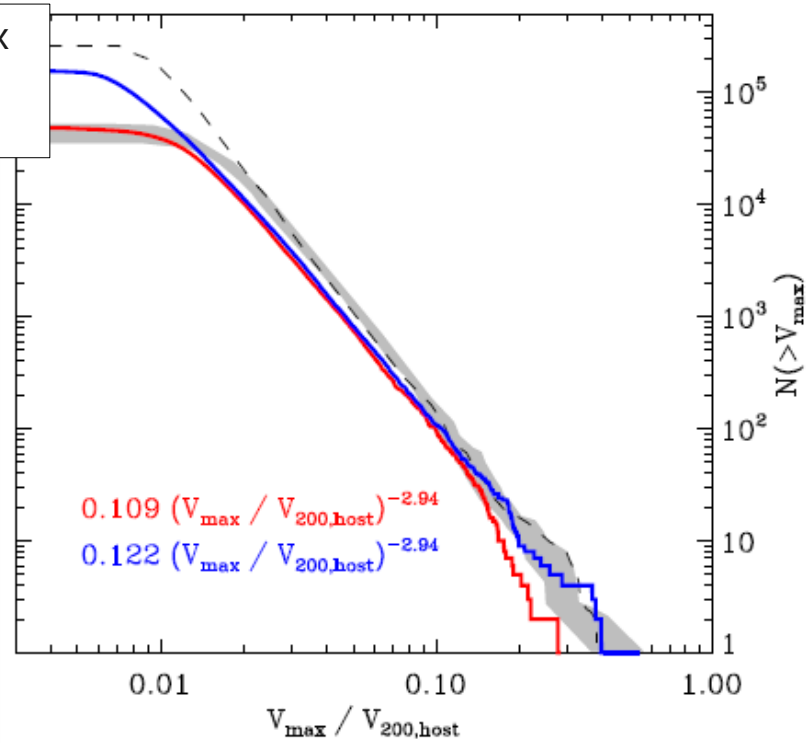

Via Lactea II, GHALO: **PKDGRAV2m**
Aquarius: **Gadget-3**

Once appropriately scaled, VL-II, GHALO, and Aquarius agree with each other.

Via Lactea II/GHALO vs. Aquarius

Some differences remain, e.g. in the radial distribution of subhalos.

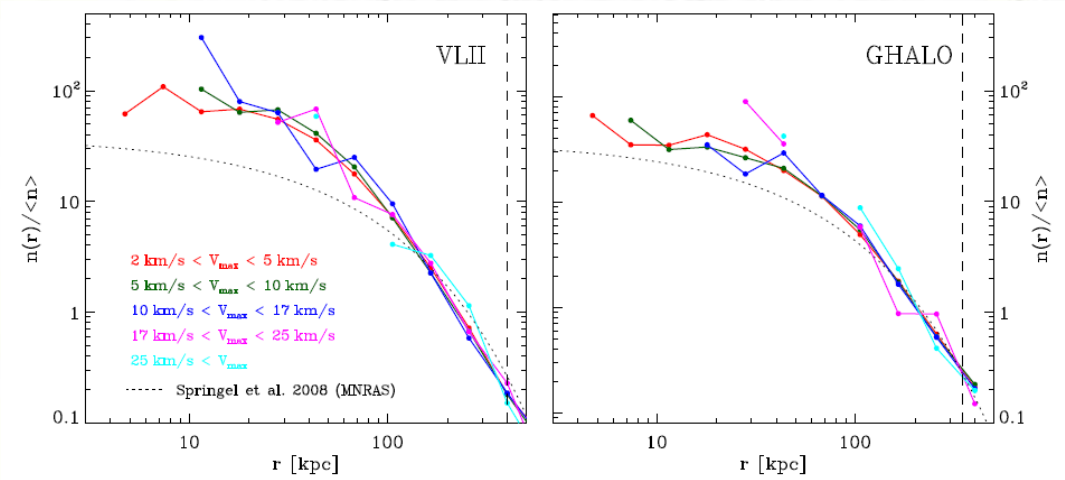

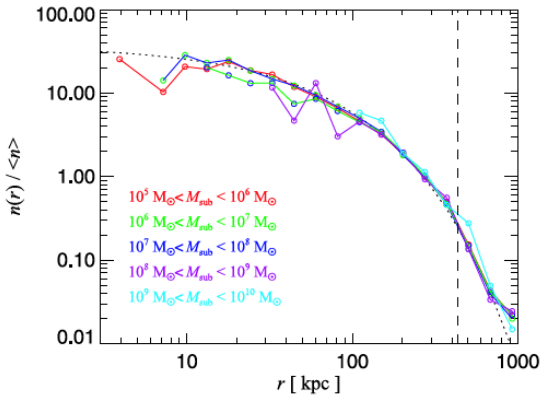

Possible explanations:

- Slightly different cosmology? σ_8=0.76, n_s=0.96 in VL2/GHALO
  σ_8=0.9, n_s=1 in Aquarius
- Different subhalo finders? 6DFOF vs. SUBFIND
- Different sample selection? V_{max} vs. M

The Radial Distribution of Subhalos Depends on Selection

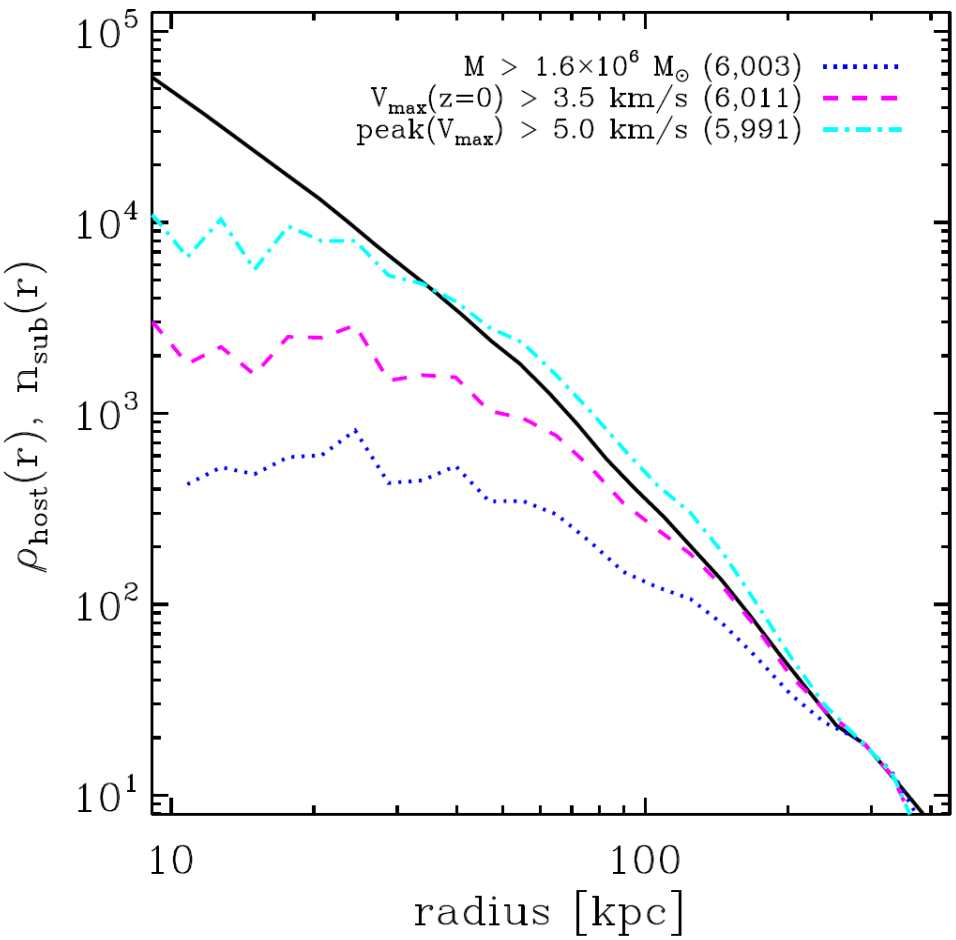

The subhalo radial distribution is **anti-biased** with respect to the DM density: fewer subhalos in the center.

(cf. Ghigna et al. 2000; de Lucia et al. 2004)

Depends on how one selection:

- strongest for M(z=0)-selected,
- weaker for Vmax(z=0)-selected,
- disappears down to ~30 kpc for peak(Vmax)-selected.

(cf. Nagai & Kravtsov 2005; Faltenbacher & Diemand 2006)

The Radial Distribution of Subhalos Depends on Selection

Subhalo n(R) normalized with Bolshoi.

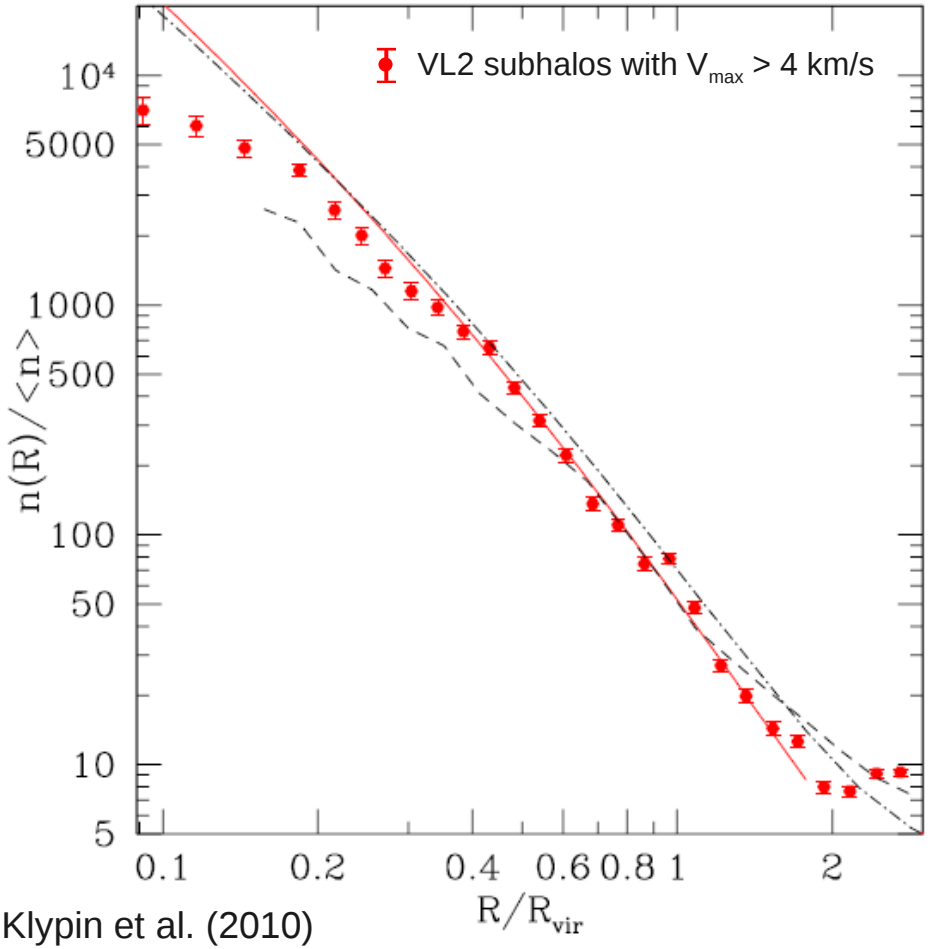

Klypin et al. (2010)

The subhalo radial distribution is **anti-biased** with respect to the DM density: fewer subhalos in the center.

(cf. Ghigna et al. 2000; de Lucia et al. 2004)

Depends on how one selection:

- strongest for M(z=0)-selected,
- weaker for Vmax(z=0)-selected,
- disappears down to ~30 kpc for peak(Vmax)-selected.

(cf. Nagai & Kravtsov 2005; Faltenbacher & Diemand 2006)

Velocity Space Substructure

Whereas previous simulations were almost completely smooth in the central region, with VL-II we resolve lots of subhalos and tidal streams even down to 8 kpc.

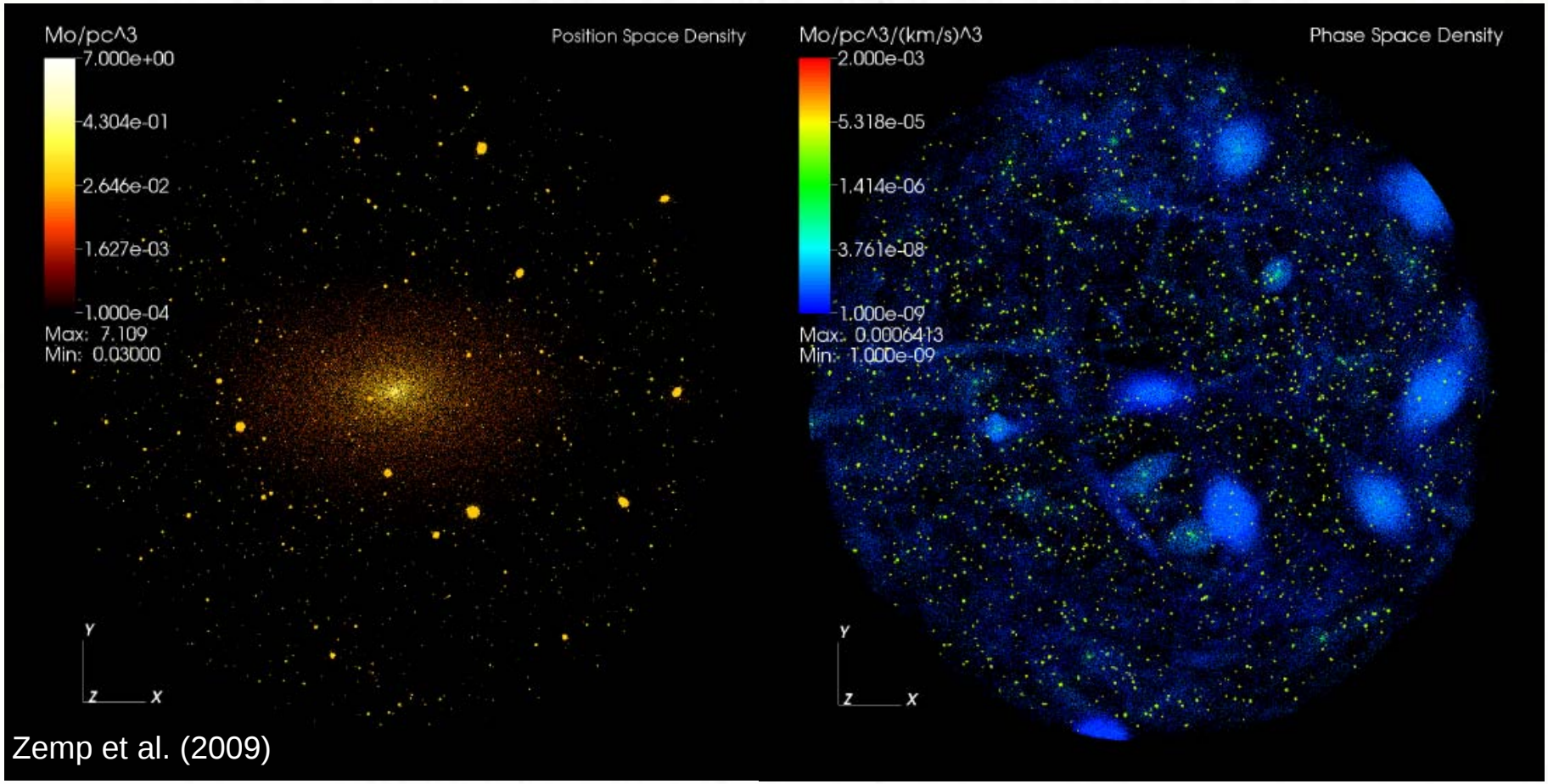

Zemp et al. (2009)

Dark Matter Substructure: Astrophysics

- Hosts for Dwarf Galaxies
  - The Missing Satellites Problem
  - How well do stellar radial velocities constrain the halo mass and the central phase space density?
  - What does this tell us about the nature of DM?
- Galactic disk bombardment
  - Heating, warps
  - Non-axisymmetric spiral structure in HI?
- Effect on cold stellar tidal streams
  - gaps, kinks?
- Effect on strong gravitational lensing:
  - Flux ratio anomalies
  - Time delay perturbations

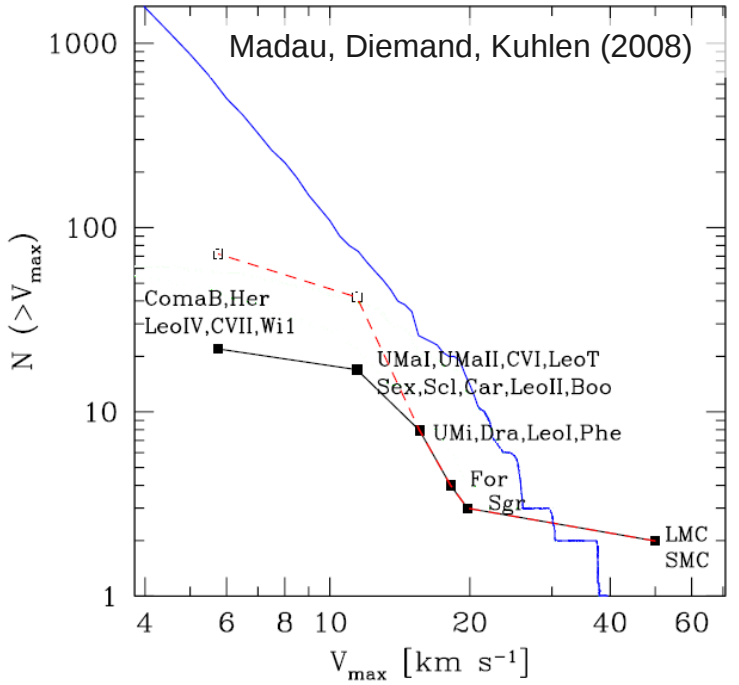

Dark Matter Substructure: Astrophysics

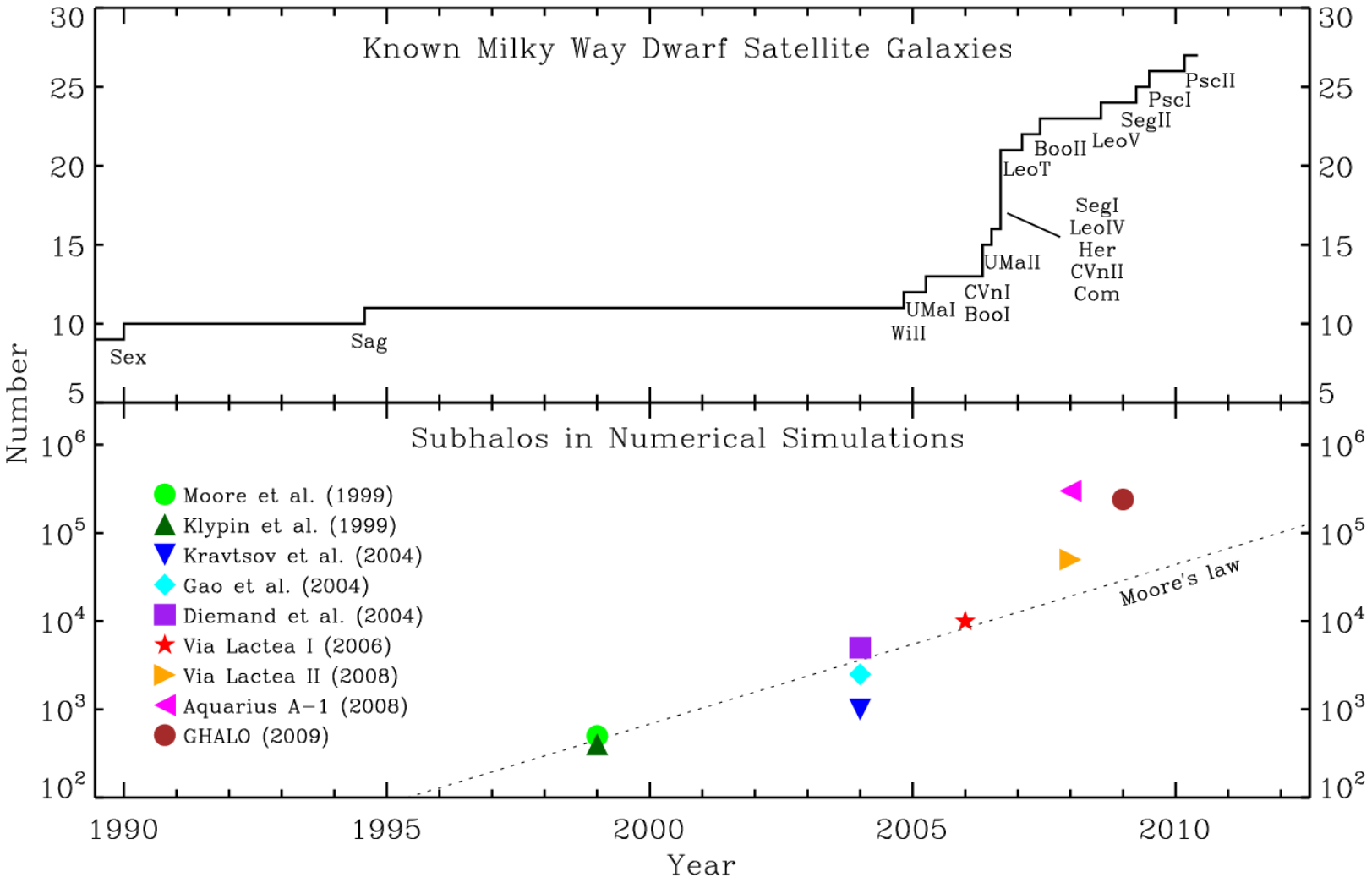

Dark Matter Substructure: Astrophysics

- Hosts for Dwarf Galaxies
  - The Missing Satellites Problem
  - How well do stellar radial velocities constrain the halo mass and the central phase space density?
  - What does this tell us about the nature of DM?
- Galactic disk bombardment
  - Heating, warps
  - Non-axisymmetric spiral structure in HI?
- Effect on cold stellar tidal streams
  - gaps, kinks?
- Effect on strong gravitational lensing:
  - Flux ratio anomalies
  - Time delay perturbations

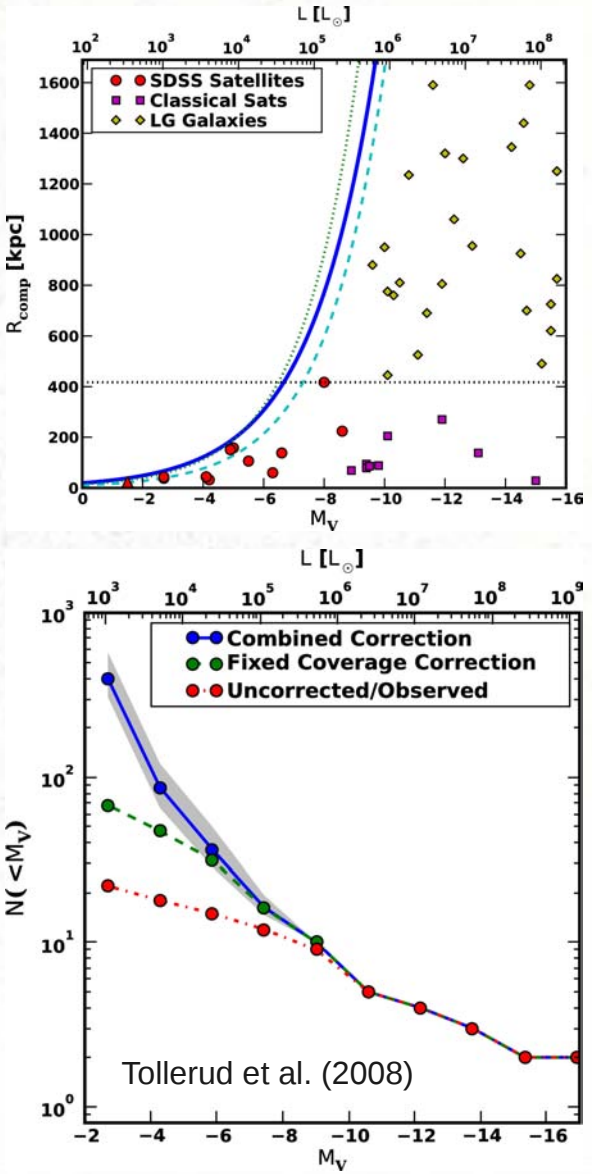

Dark Matter Substructure: Astrophysics

- Hosts for Dwarf Galaxies
  - The Missing Satellites Problem
  - How well do stellar radial velocities constrain the halo mass and the central phase space density?
  - What does this tell us about the nature of DM?
- Galactic disk bombardment
  - Heating, warps
  - Non-axisymmetric spiral structure in HI?
- Effect on cold stellar tidal streams
  - gaps, kinks?
- Effect on strong gravitational lensing:
  - Flux ratio anomalies
  - Time delay perturbations

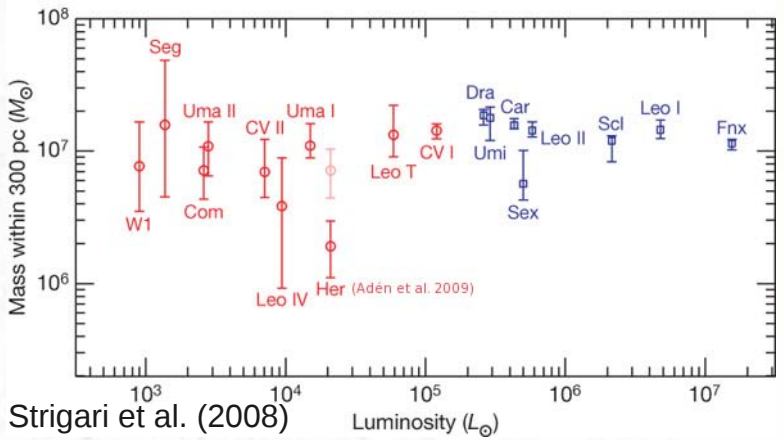

Strigari et al. (2008)

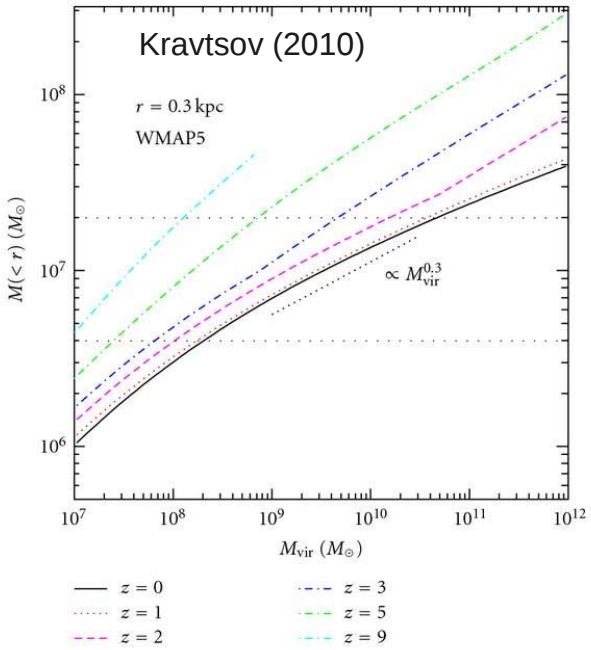

Dark Matter Substructure: Astrophysics

- Hosts for Dwarf Galaxies
  - The Missing Satellites Problem
  - How well do stellar radial velocities constrain the halo mass and the central phase space density?
  - What does this tell us about the nature of DM?
- Galactic disk bombardment
  - Heating, warps
  - Non-axisymmetric spiral structure in HI?
- Effect on cold stellar tidal streams
  - gaps, kinks?
- Effect on strong gravitational lensing:
  - Flux ratio anomalies
  - Time delay perturbations

Levine, Blitz, & Heiles (2006)

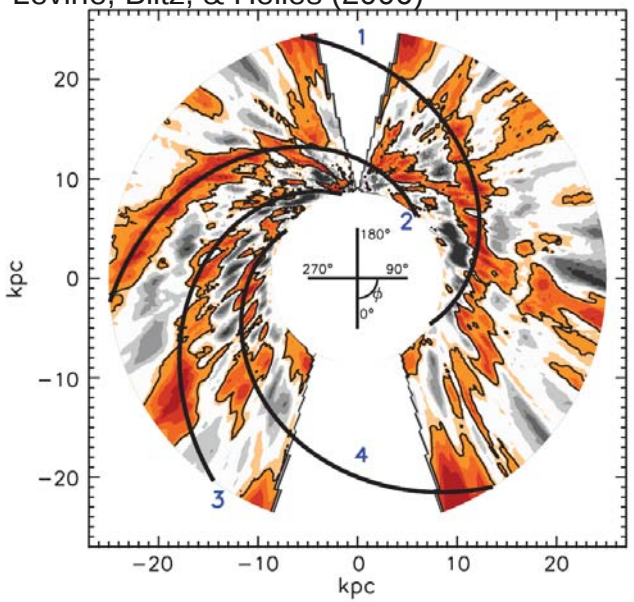

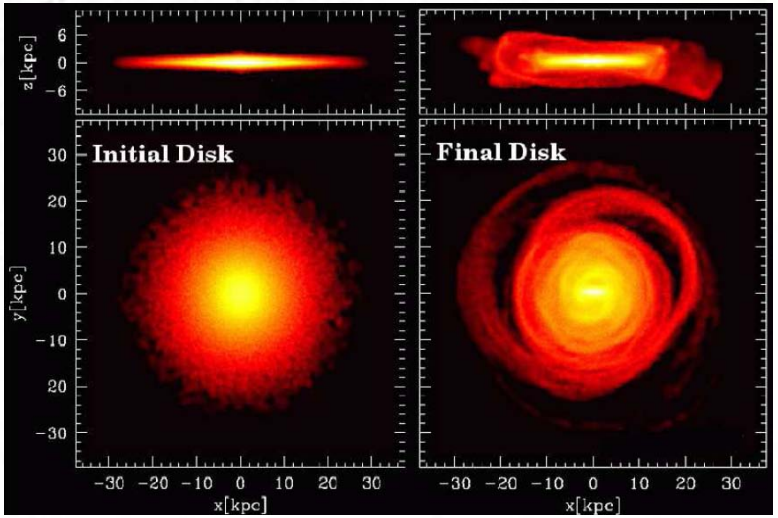

Kazantzidis et al. (2010)

Dark Matter Substructure: Astrophysics

- Hosts for Dwarf Galaxies
  - The Missing Satellites Problem
  - How well do stellar radial velocities constrain the halo mass and the central phase space density?
  - What does this tell us about the nature of DM?
- Galactic disk bombardment
  - Heating, warps
  - Non-axisymmetric spiral structure in HI?
- Effect on cold stellar tidal streams
  - gaps, kinks?
- Effect on strong gravitational lensing:
  - Flux ratio anomalies
  - Time delay perturbations

Grillmair & Dinatos (2006)

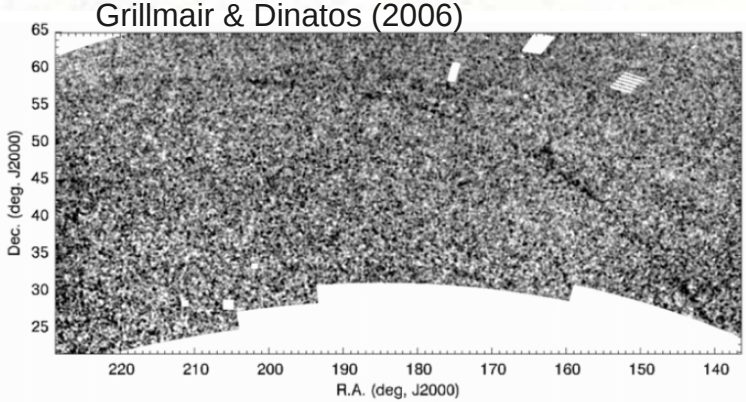

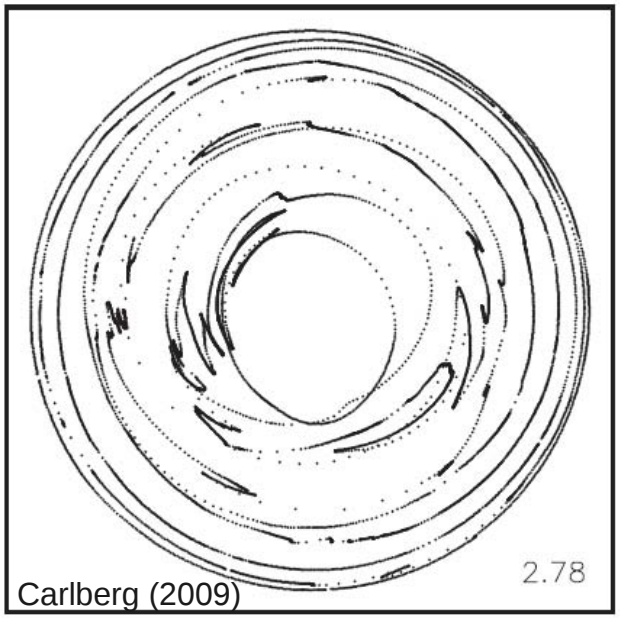

Carlberg (2009)

Dark Matter Substructure: Astrophysics

- Hosts for Dwarf Galaxies
  - The Missing Satellites Problem
  - How well do stellar radial velocities constrain the halo mass and the central phase space density?
  - What does this tell us about the nature of DM?
- Galactic disk bombardment
  - Heating, warps
  - Non-axisymmetric spiral structure in HI?
- Effect on cold stellar tidal streams
  - gaps, kinks?
- Effect on strong gravitational lensing
  - Flux ratio anomalies
  - Time delay perturbations

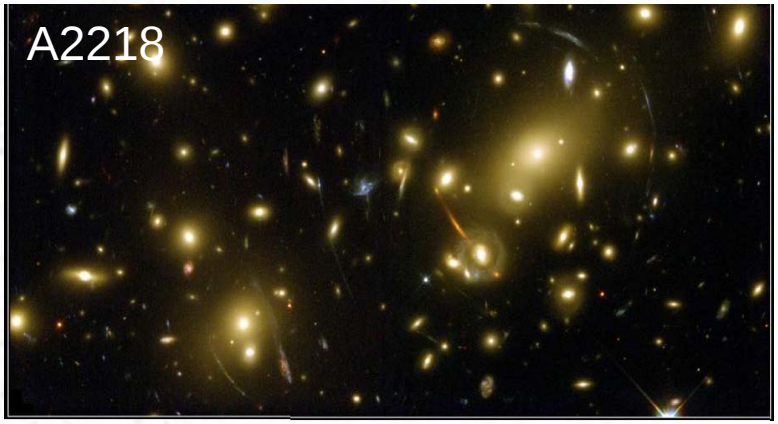

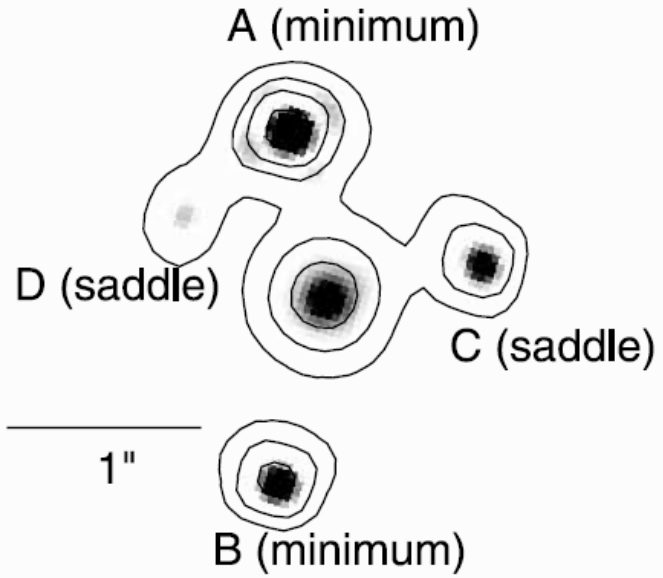

Kochanek & Dalal (2004)

Dark Matter Substructure: Particle Physics

1) Subhalos as individual DM annihilation sources
   a) Luminous dwarf satellite galaxies
   b) Dark subhalos
2) Cumulative signal from all Galactic subhalos
3) Substructure “boost factor”
4) Velocity substructure and Direct Detection

DM annihilation and its signals

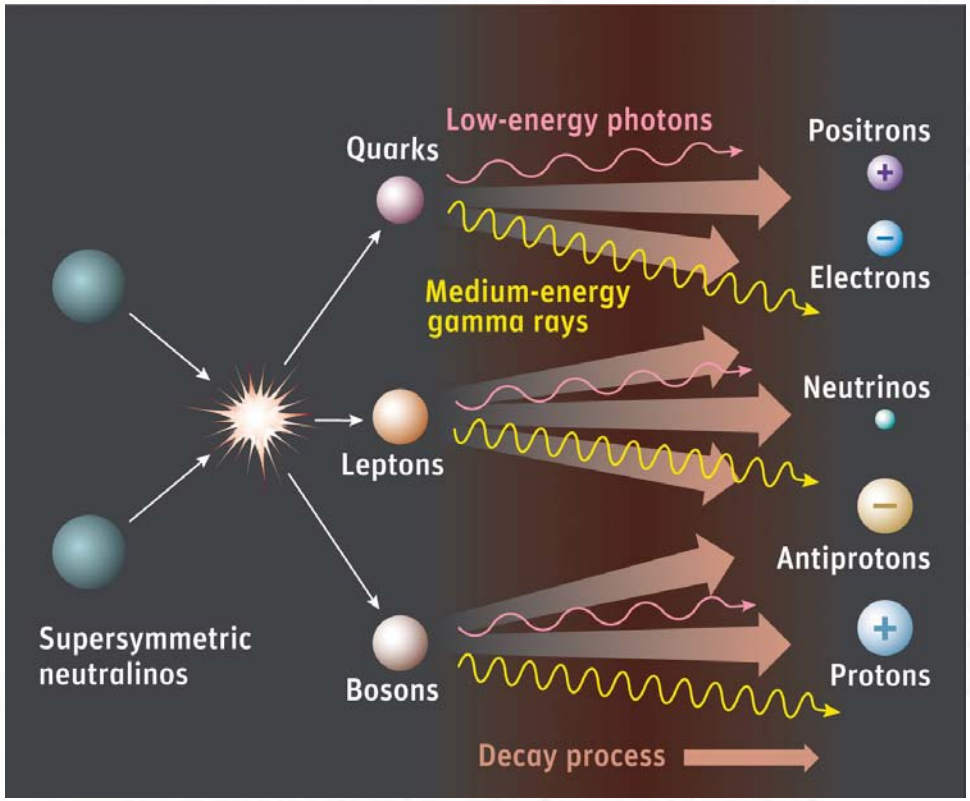

PAMELA satellite

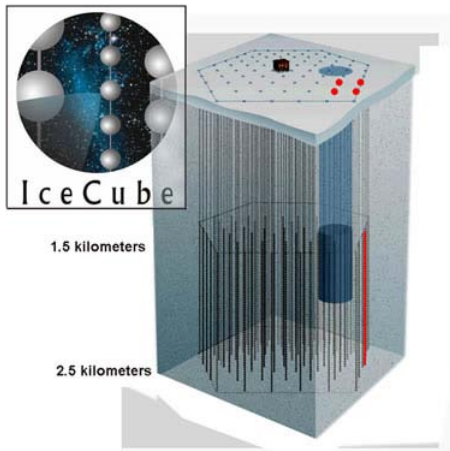

1) Subhalos as individual DM annihilation sources

$$N_\gamma = \left[\int_{\text{line of sight}} \rho^2_{\text{DM}}\, dl(\psi)\right] \frac{\langle\sigma v\rangle}{2M_\chi^2} \left[\int_{E_{th}}^{M_\chi} \left(\frac{dN_\gamma}{dE}\right) A_{\text{eff}}(E) dE\right] \frac{\Delta\Omega}{4\pi}\, \tau_{\text{exp}}$$

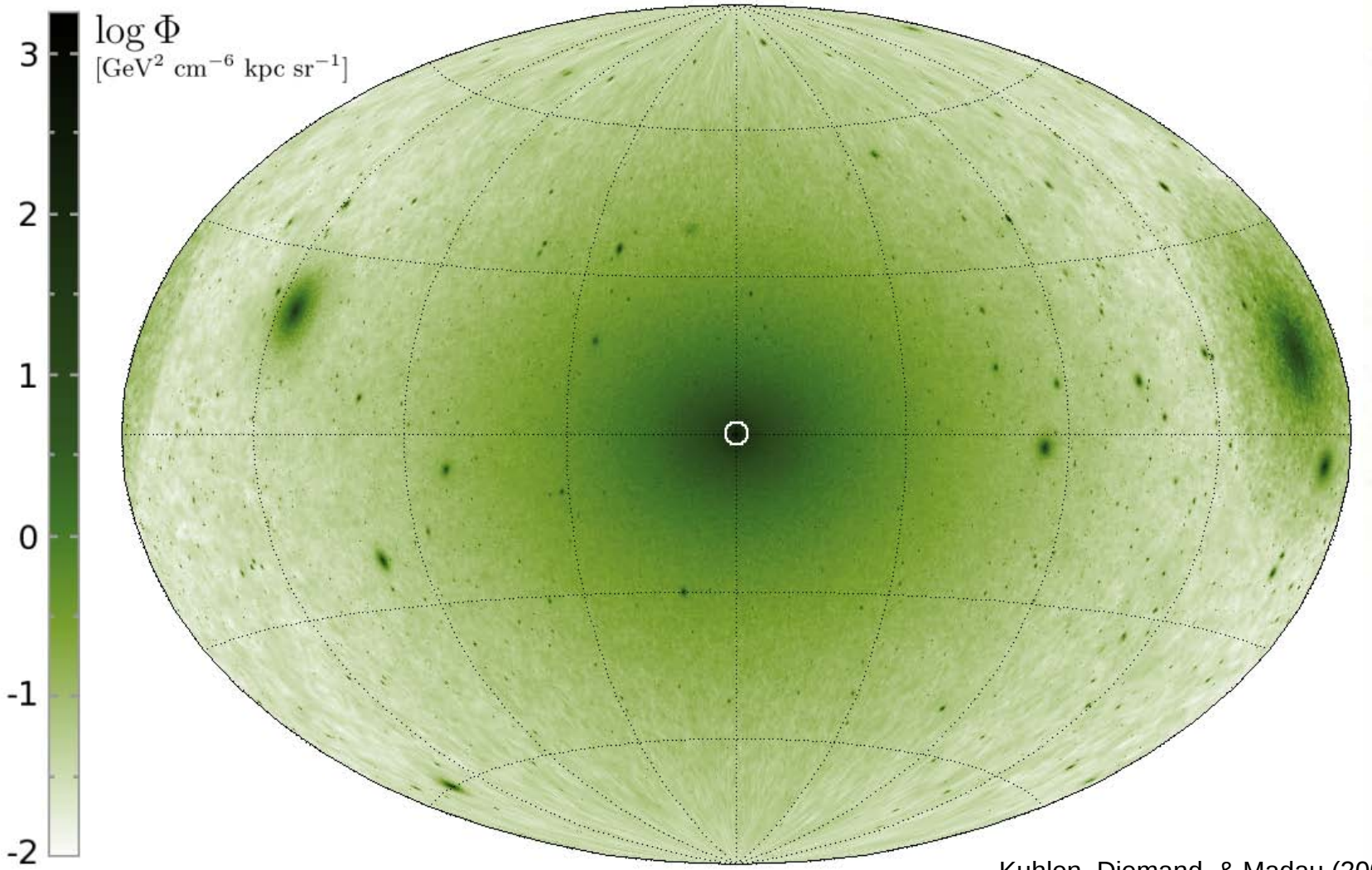

Kuhlen, Diemand, & Madau (2008)

1) Subhalos as individual DM annihilation sources

$$N_\gamma = \left[\int_{\text{line of sight}} \rho^2_{\text{DM}}\, dl(\psi)\right] \frac{\langle\sigma v\rangle}{2M_\chi^2} \left[\int_{E_{th}}^{M_\chi} \left(\frac{dN_\gamma}{dE}\right) A_{\text{eff}}(E) dE\right] \frac{\Delta\Omega}{4\pi}\, \tau_{\text{exp}}$$

Huh? How come these look so different?

Via Lactea II

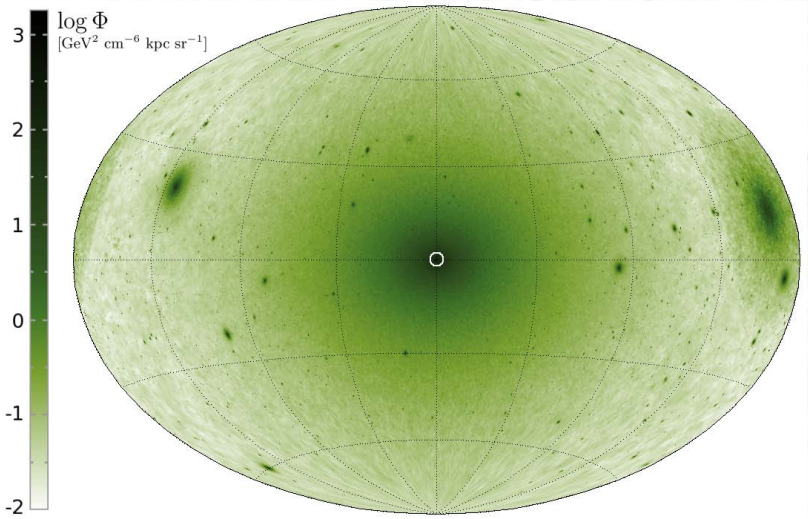

Kuhlen, Diemand, & Madau (2008)

Aquarius

Springel et al. (2008)

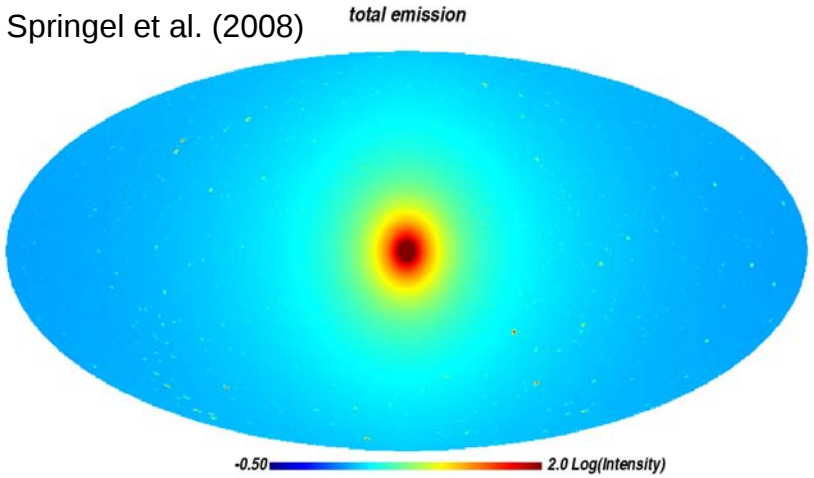

“For simplicity and for better visual representation they [the subhalos] have been represented as point sources that were smoothed with a Gaussian beam of 40 arcmin.”

1) Subhalos as individual DM annihilation sources

Fermi/LAT *GTOBSSIM* Monte-Carlo Simulation (with Brandon Anderson & Robert Johnson, SCIPP)

- LAT A_{eff} dependence on viewing angle and photon energy
- Selection effects: LAT trigger, on-board filter, offline analysis to reject cosmic-rays
- PSF includes non-Gaussian tails
- Thin and thick tungsten foils treated separately
- $\pm 35^{\circ}$ instrument rocking
- South Atlantic Anomaly Passage dead time

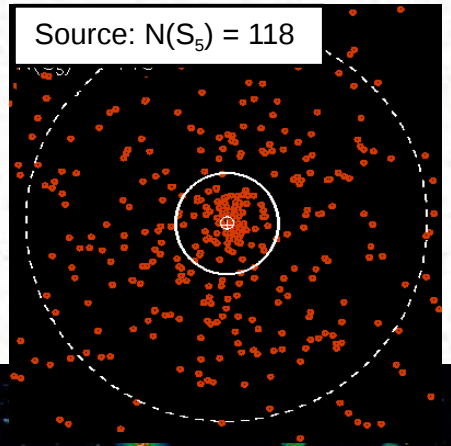

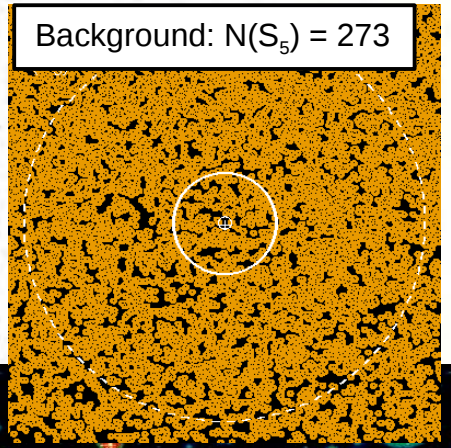

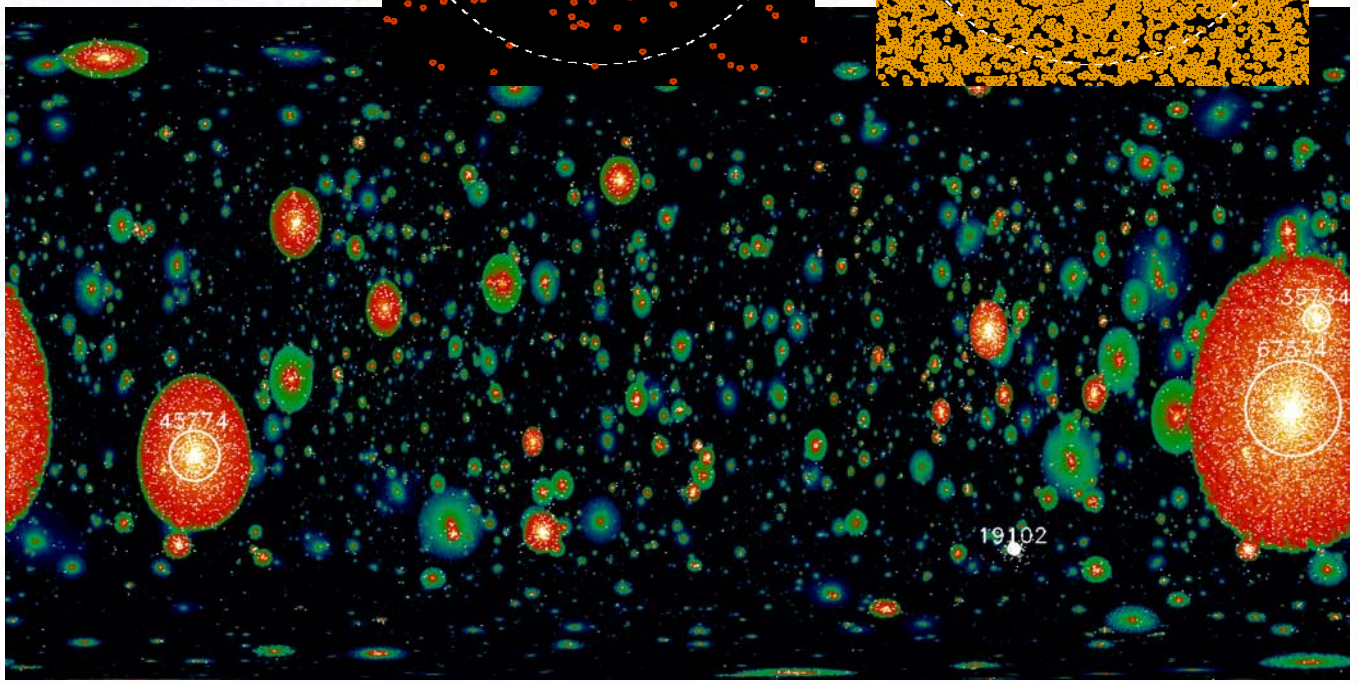

Energy-dependent ROI optimization

Calculate detection significance:

$$P = \sum_{i=k}^{\infty} \frac{\lambda^k e^{-\lambda}}{k!}$$

$$S = \sqrt{2}\ \mathrm{erf}^{-1}(1 - 2\mathrm{P})$$

1) Subhalos as individual DM annihilation sources

Fermi/LAT *GTOBSSIM* Monte-Carlo Simulation (with Brandon Anderson & Robert Johnson, SCIPP)

- LAT A_{eff} dependence on viewing angle and photon energy
- Selection effects: LAT trigger, on-board filter, offline analysis to reject cosmic-rays
- PSF includes non-Gaussian tails
- Thin and thick tungsten foils treate
  separately
- $\pm 35^{\circ}$ instrument rocking
- South Atlantic Anomaly Passage c

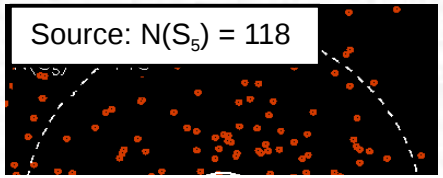

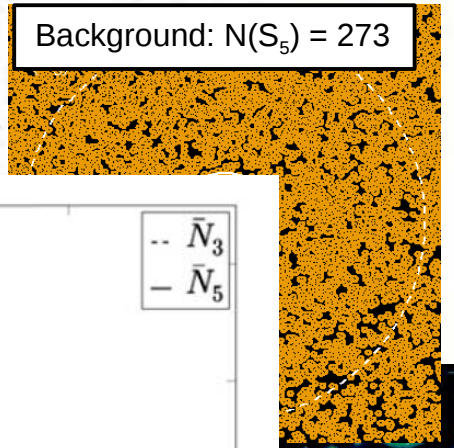

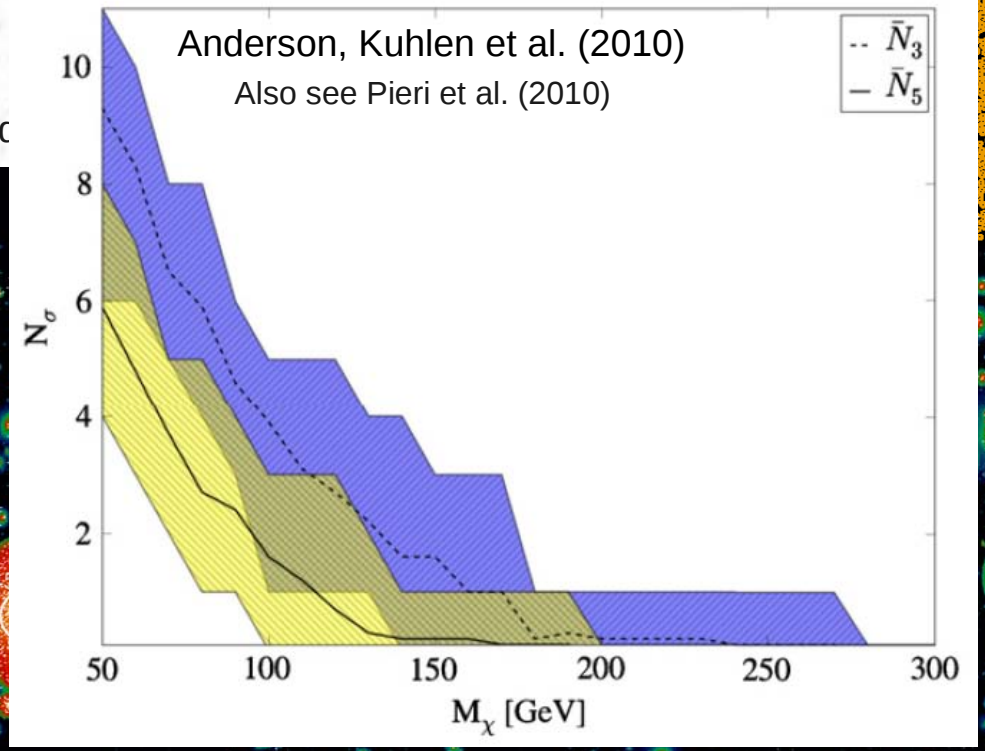

Energy-dependent ROI optimization

Calculate detection significance:

$$P = \sum_{i=k}^{\infty} \frac{\lambda^k e^{-\lambda}}{k!}$$

$$S = \sqrt{2}\ \mathrm{erf}^{-1}(1 - 2\mathrm{P})$$

1) Subhalos as individual DM annihilation sources

Fermi was launched on June 11th 2008 and has been observing the sky for more than 2 years.

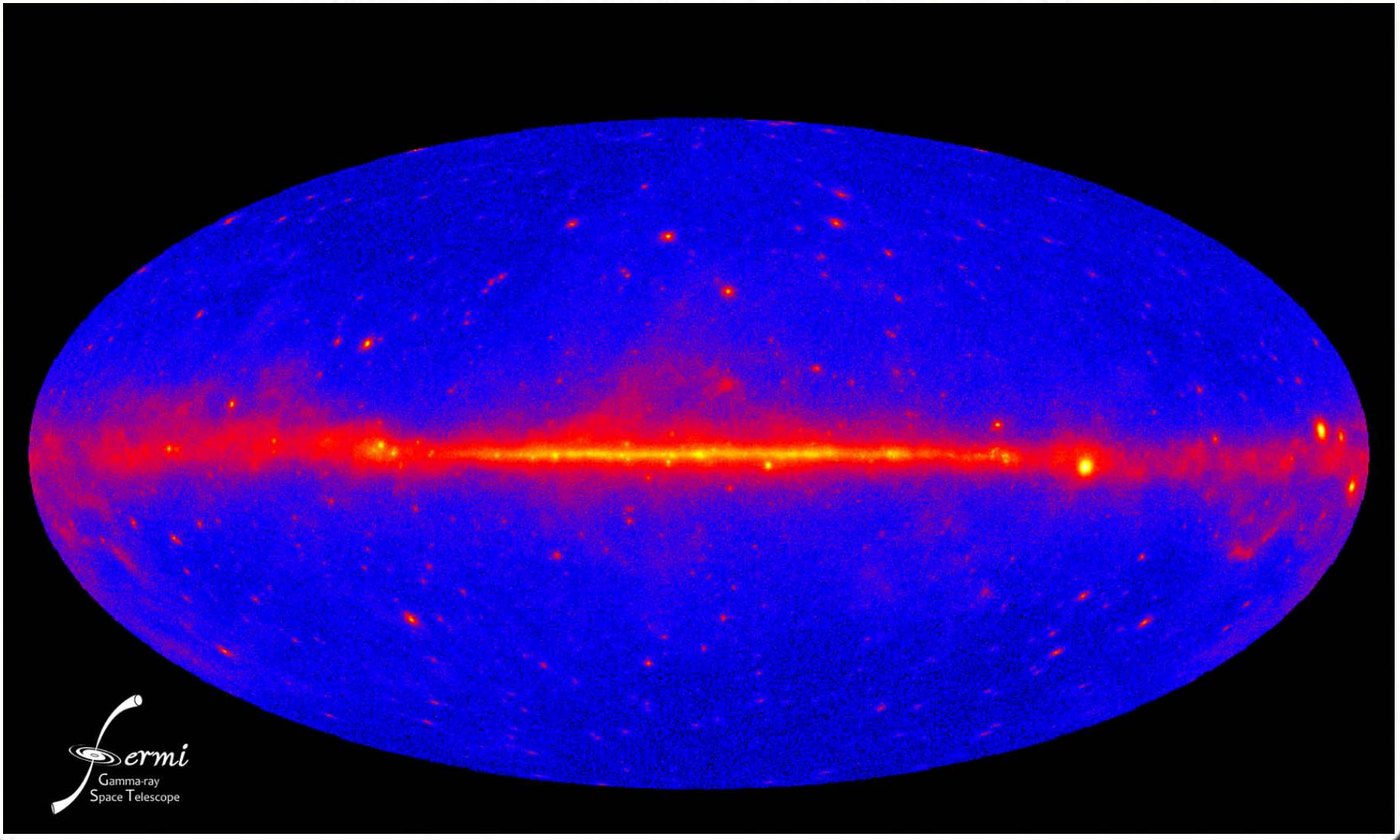

1) Subhalos as individual DM annihilation sources

So far, now dark matter signal has been detected. ☹

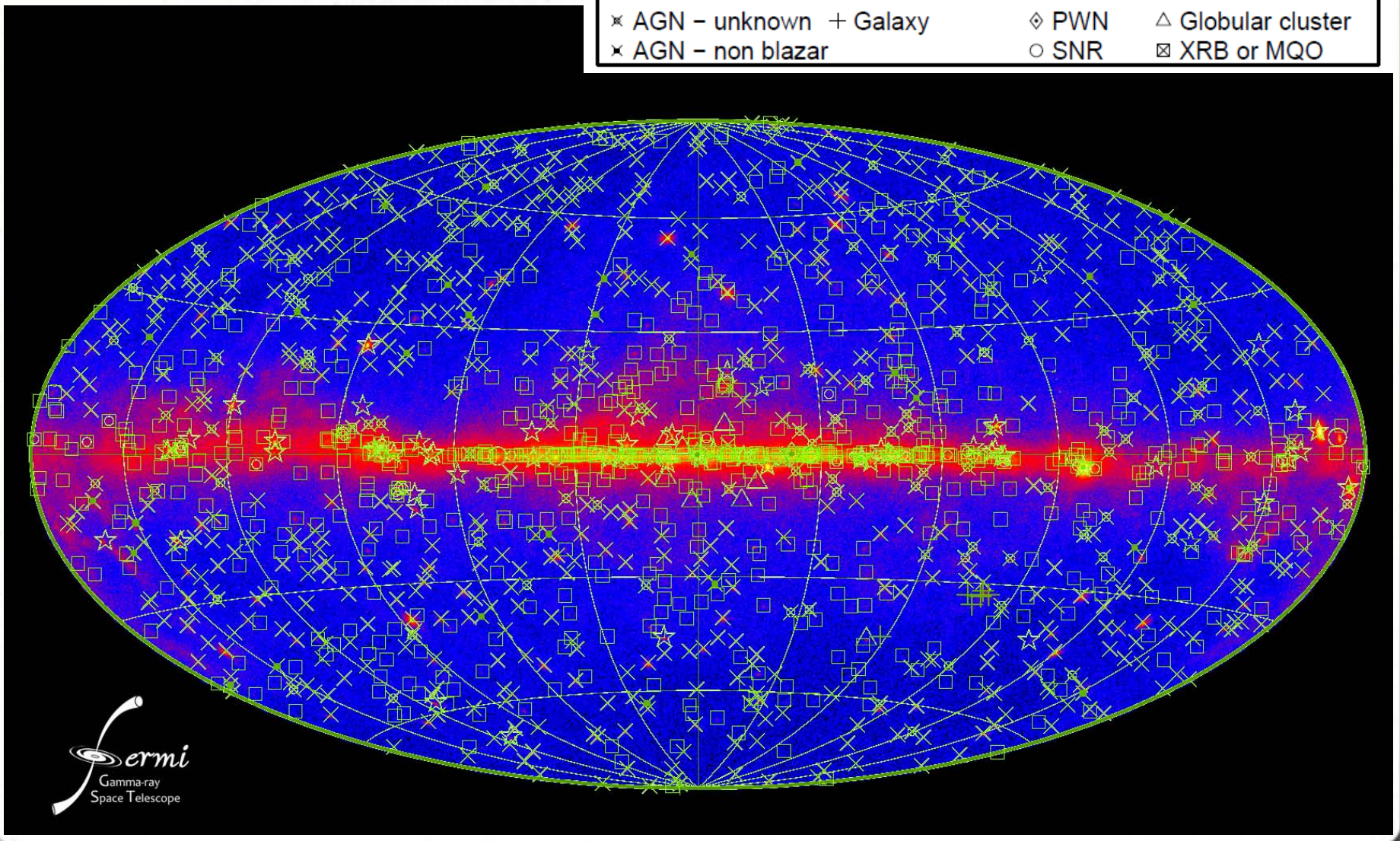

1) Subhalos as individual DM annihilation sources

Luminous dwarf satellite galaxies

- Know where to look
- Can stack data
- Targeted observations with ACTs
- Distance known ➞ better constraints

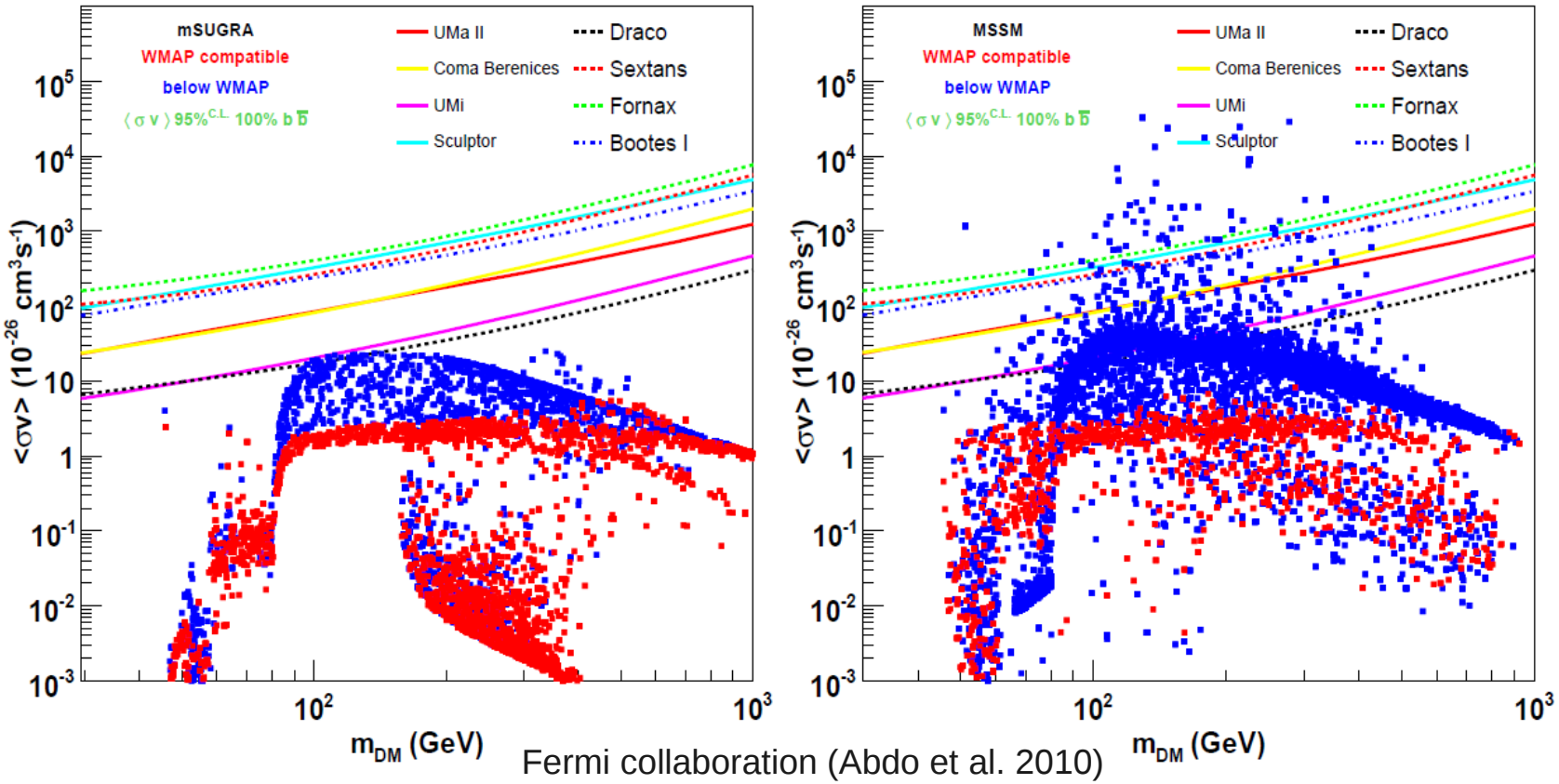

Fermi collaboration (Abdo et al. 2010)

1) Subhalos as individual DM annihilation sources

Dark Subhalos

- Need a large area survey
- Could in principle be very nearby
- Less confusion from astrophysical sources

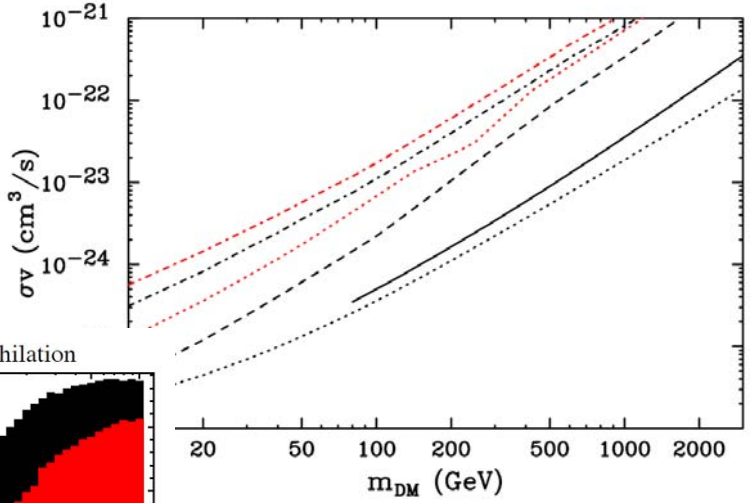

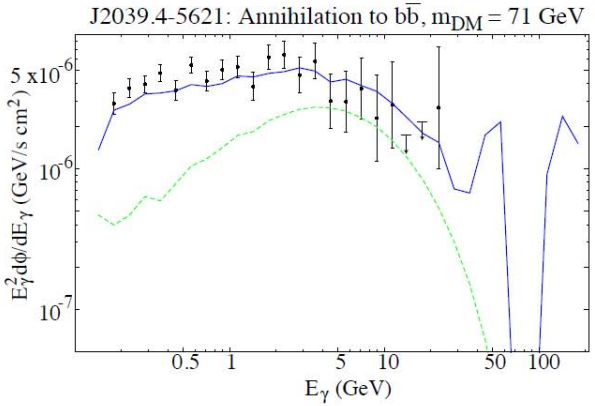

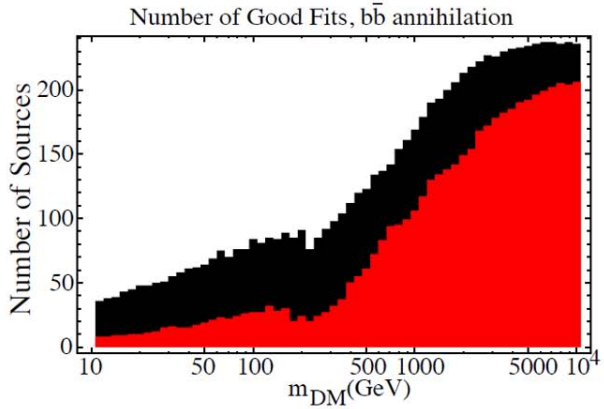

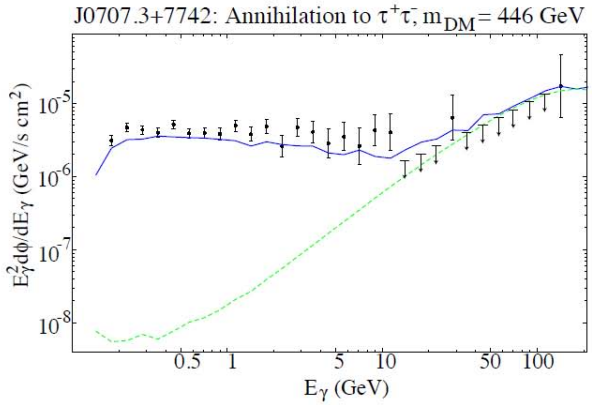

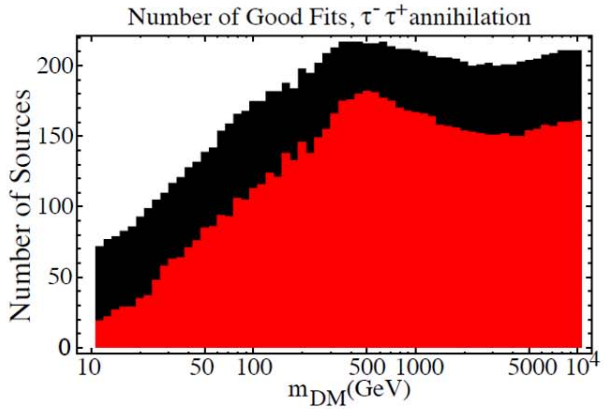

Buckley & Hooper (2010)

- Searched FGST point source catalog
- No definite detections
- Limits competitive with those from dwarf galaxies
- ~30 subhalos could be hiding as point sources

2) Cumulative signal from all Galactic subhalos

SUBHALO MASS FUNCTION MODELS

α	m_0 ($M_\odot$)	$N_{\rm tot}$	$M_{\rm tot}$ ($M_\odot$)	$f_{\rm tot}$	M_u ($M_\odot$)	f_u
2.0.....	10^{-6}	2.5×10^{16}	9.3×10^{11}	0.53	7.0×10^{11}	0.40
1.9.....	10^{-6}	9.2×10^{14}	3.2×10^{11}	0.19	1.2×10^{11}	0.070
1.8.....	10^{-6}	3.3×10^{13}	2.1×10^{11}	0.12	3.3×10^{10}	0.018
2.0.....	1	2.5×10^{10}	5.8×10^{11}	0.33	3.5×10^{11}	0.20
2.0.....	10^{-12}	2.5×10^{22}	1.3×10^{12}	0.73	1.0×10^{12}	0.60

- CDM predicts an enormous number of low mass subhalos.
- Their cumulative annihilation signal should result in a diffuse flux.
- Less centrally concentrated than the host halo flux.
- Reduced contrast between center and anti-center. Bad news for IceCube? (Rott et al. 2010)
- Angular fluctuations are an interesting signal to be searched for (Siegal-Gaskins et al. 2008, Ando 2009)

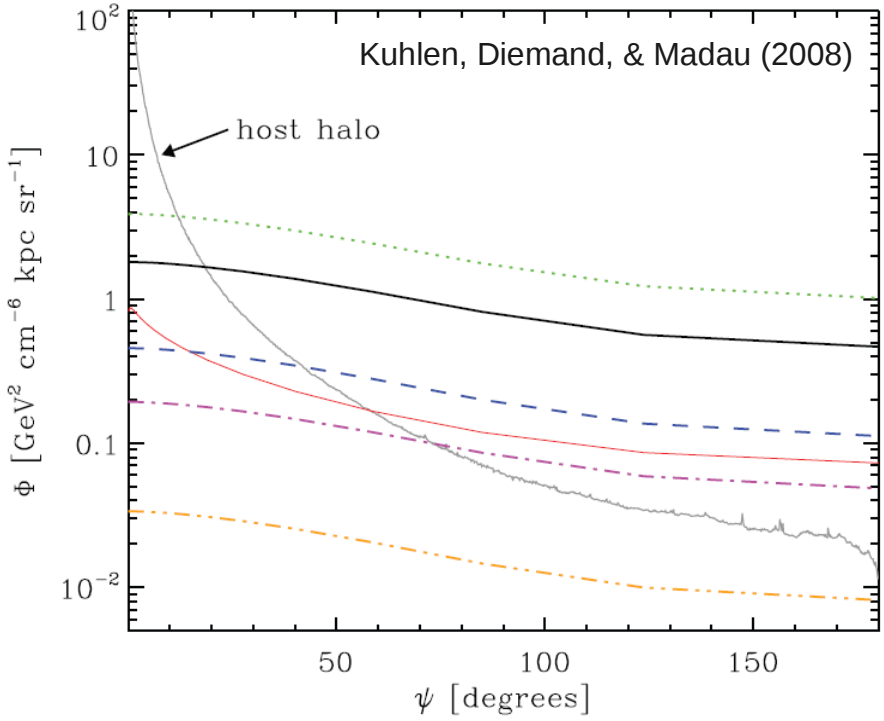

3) Substructure “Boost Factor”

The term “Boost Factor” has been used (abused?) in many ways:

- Enhancement in total halo luminosity from NFW profile compared to a spherical tophat.
- Enhancement in total halo luminosity from substructure (and sub-substructure, etc.) compared to a smooth NFW density profile.
- Enhancement of local (8kpc) annihilation rate over $(0.3\ \mathrm{GeV\ cm^{-3}})^2$.
- Enhancement of Galactic Center annihilation rate.
- Enhancement of the surface brightness of angularly resolved subhalos.

There is no one single “Boost Factor”!

The enhancement due to clumpy substructure depends on source location and/or its angular extent.

3) Substructure “Boost Factor”

Total Halo Luminosity Boost Factor

- Only applicable to unresolved sources!
- Important for the extragalactic gamma-ray background

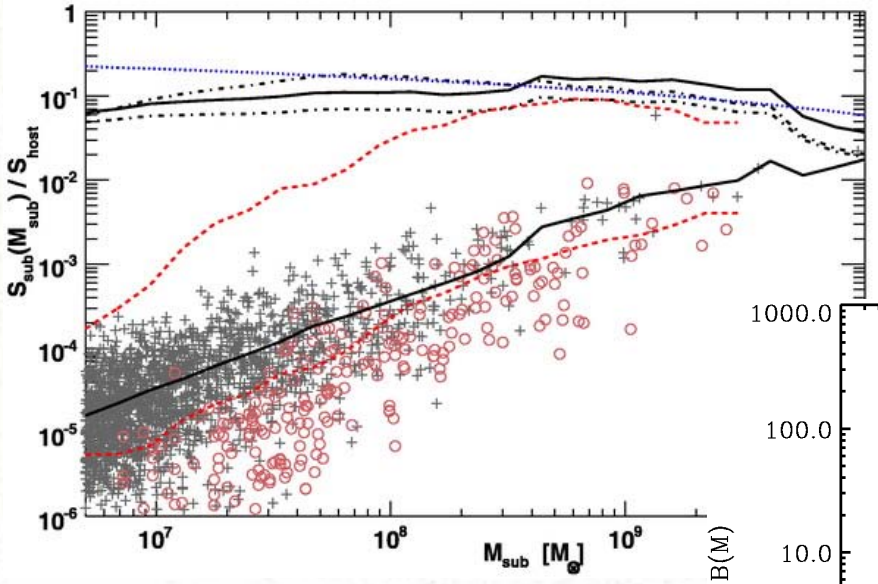

Diemand, Kuhlen, & Madau (2006) [VL-I]

$$\mathcal{L}(M) = [1 + B(M, m_0)]\tilde{\mathcal{L}}(M)$$

$$B(M) = \frac{A}{\tilde{L}(M)} \int_{\ln m_0}^{\ln m_1} \left(\frac{m}{M}\right)^{1-\alpha} [1 + B(m)]\, \tilde{L}(m) d\ln m.$$

Kuhlen, Diemand, & Madau (2008)

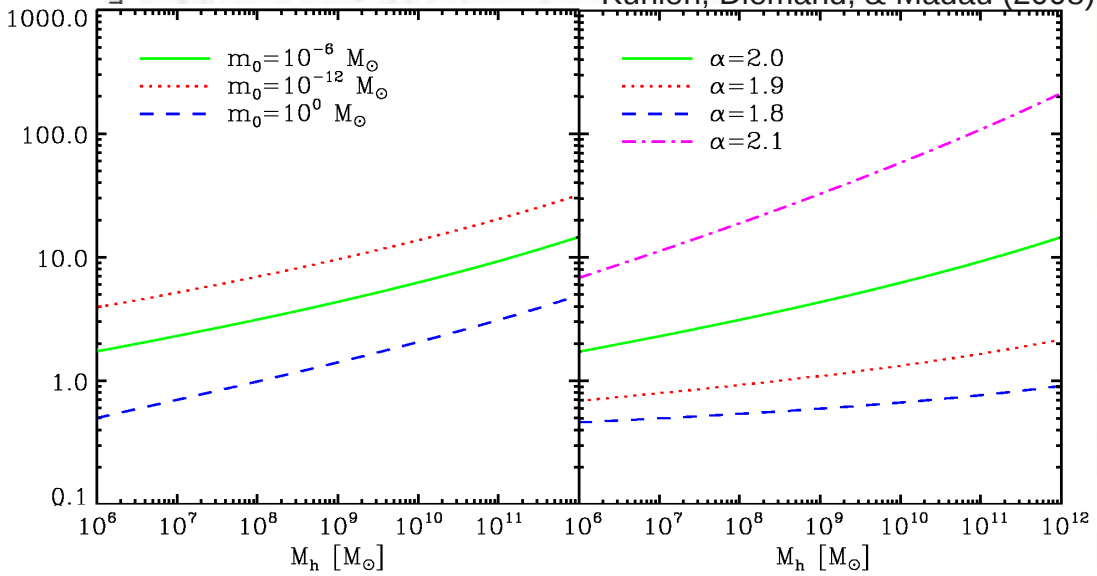

3) Substructure “Boost Factor”

Total Halo Luminosity Boost Factor

- Only applicable to unresolved sources!
- Important for the extragalactic gamma-ray background.

Springel et al. (2008)

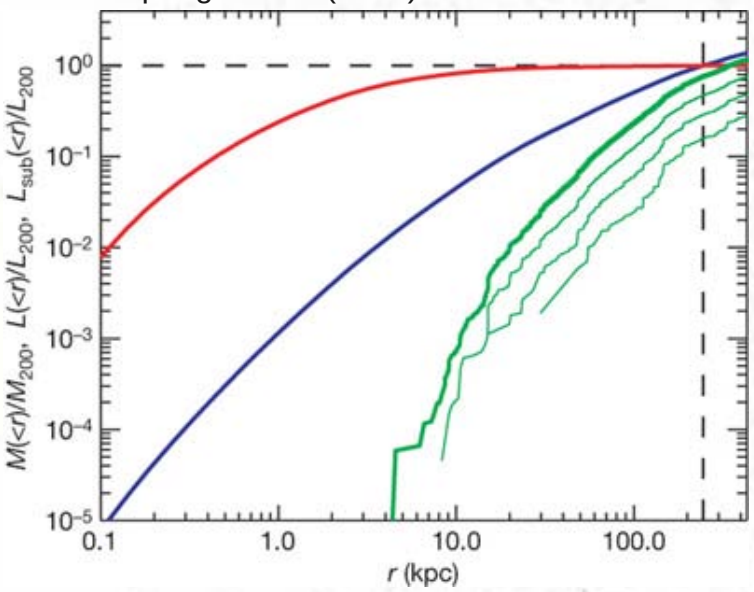

$L(>M_{min}) \sim M_{min}^{-0.226}$

Total boost factor for $M_{min}=10^{-6}\ M_{\odot}$ = 232!

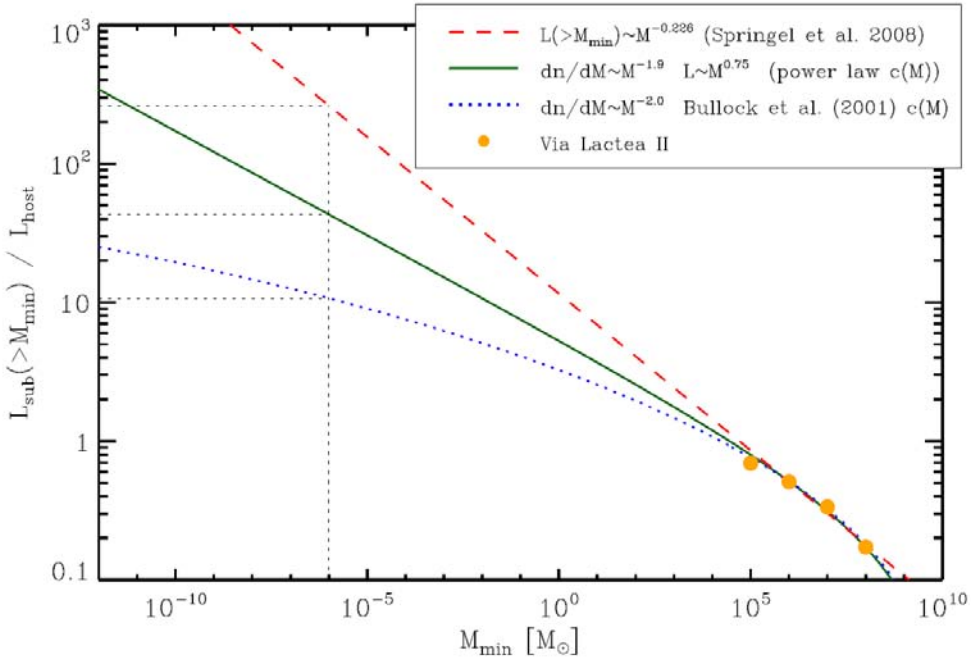

Depends **critically** on what one assumes for the concentration-mass relation for subhalos below the simulations' resolution limit!

3) Substructure “Boost Factor”

$$P(\rho; r) = \frac{f_s}{\sqrt{2\pi\Delta^2}} \frac{1}{\rho} \exp\left\{ -\frac{1}{2\Delta^2} \left[\ln\left(\frac{\rho}{\rho_h} e^{\Delta^2/2} \right) \right]^2 \right\} + (1 - f_s) \frac{1 + \alpha(r)}{\rho_h} \Theta(\rho - \rho_h) \left(\frac{\rho}{\rho_h} \right)^{-(2+\alpha)}$$

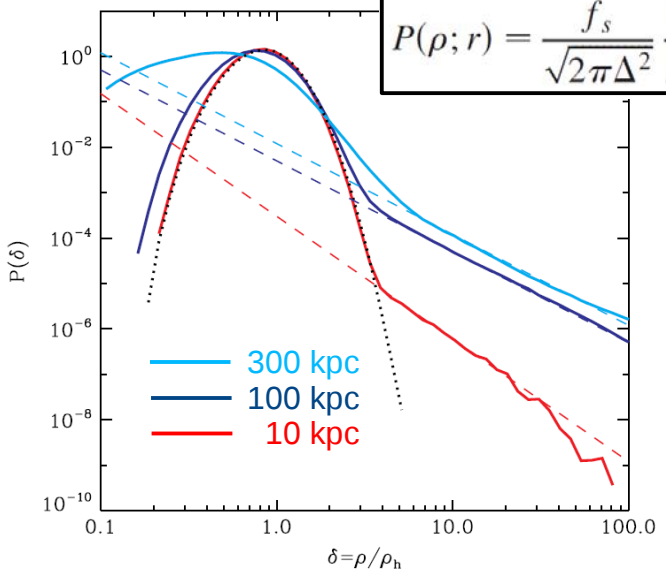

- We measure the PDF of ρ/ρ_{host} in the simulation.
- It's fit well by a **log-normal** plus a **powerlaw** tail due to substructure.

$$\alpha \approx 0.0 \pm 0.1 \qquad 1 - f_s(r) = 7 \times 10^{-3} \left(\frac{\bar{\rho}(r)}{\bar{\rho}(r = 100 \text{ kpc})} \right)^{-0.26}$$

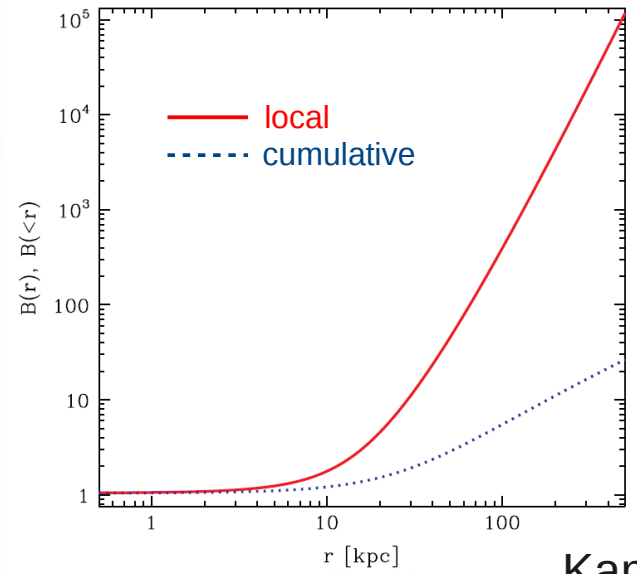

$$B(r) = \frac{\int \rho^2 dV}{\int [\bar{\rho}(r)]^2 dV} = \int_0^{\rho_{\max}} P(\rho, r) \frac{\rho^2}{[\bar{\rho}(r)]^2} d\rho$$

$$B(r) = f_s e^{\Delta^2} + (1 - f_s) \frac{1 + \alpha}{1 - \alpha} \left[\left(\frac{\rho_{\max}}{\rho_h} \right)^{1-\alpha} - 1 \right]$$

Local boost (e.g. at 8 kpc or at the G.C.) ≠ Total boost

Kamionkowski, Koushiappas & Kuhlen (2010)

3) Substructure “Boost Factor”

$$P(\rho; r) = \frac{f_s}{\sqrt{2\pi\Delta^2}} \frac{1}{\rho} \exp\left\{-\frac{1}{2\Delta^2}\left[\ln\left(\frac{\rho}{\rho_h} e^{\Delta^2/2}\right)\right]^2\right\} + (1 - f_s)\frac{1+\alpha(r)}{\rho_h}\Theta(\rho - \rho_h)\left(\frac{\rho}{\rho_h}\right)^{-(2+\alpha)}$$

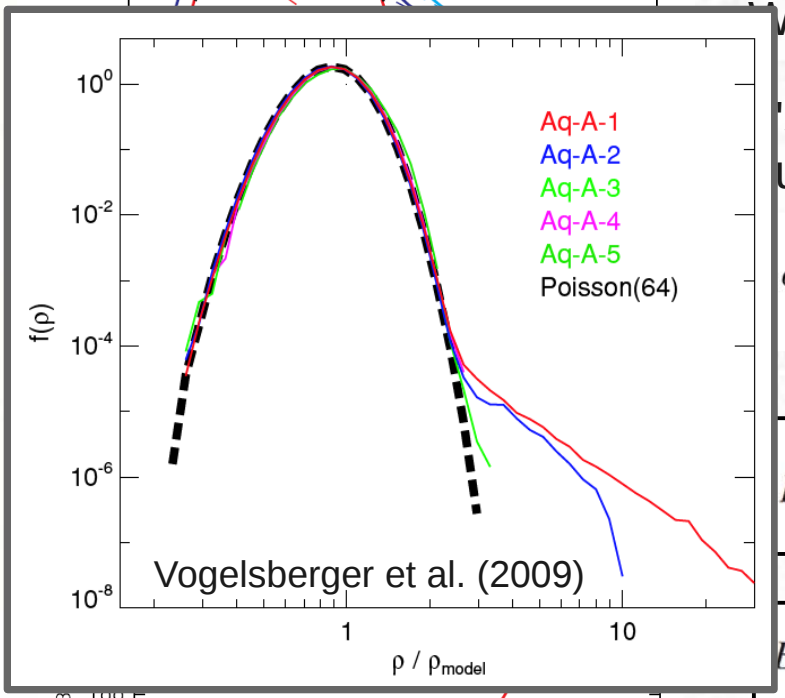

We measure the PDF of ρ/ρ_{host} in the simulation.

It's fit well by a **log-normal** plus a **powerlaw** tail due to substructure.

$$\alpha \approx 0.0 \pm 0.1 \qquad 1 - f_s(r) = 7 \times 10^{-3}\left(\frac{\bar{\rho}(r)}{\bar{\rho}(r = 100\ \mathrm{kpc})}\right)^{-0.26}$$

$$B(r) = \frac{\int \rho^2 dV}{\int [\bar{\rho}(r)]^2 dV} = \int_0^{\rho_{max}} P(\rho, r)\frac{\rho^2}{[\bar{\rho}(r)]^2} d\rho$$

$$B(r) = f_s e^{\Delta^2} + (1 - f_s)\frac{1+\alpha}{1-\alpha}\left[\left(\frac{\rho_{max}}{\rho_h}\right)^{1-\alpha} - 1\right]$$

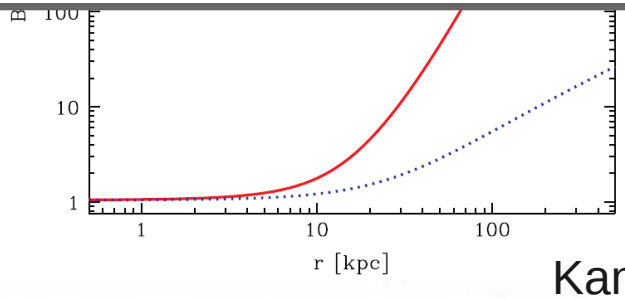

Local boost (e.g. at 8 kpc or at the G.C.) ≠ Total boost

Kamionkowski, Koushiappas & Kuhlen (2010)

4) Substructure And Direct Detection

Cryogenic phonon detection (e.g. CDMS)

Liquid Xenon scintillation detectors (e.g. Xenon100, LUX)

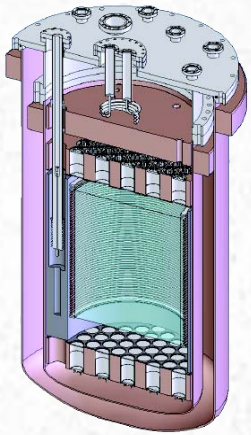

Directionally sensitive (e.g. DRIFT, DMTPC)

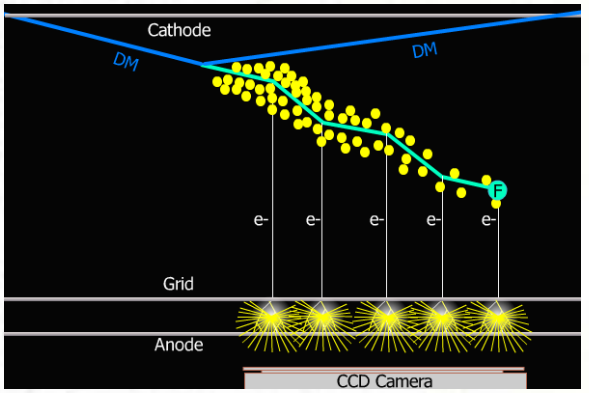

$$\frac{dR}{dE_R} = N_T M_N \frac{\rho_\chi \sigma_n}{2 m_\chi \mu_{ne}^2} \frac{(f_p Z + f_n (A - Z))^2}{f_n^2} F^2[E_R] \int_{\beta_{min}}^{\infty} \frac{f(v)}{v} dv$$

4) Substructure And Direct Detection

Cryogenic phonon detection (e.g. CDMS)

Liquid Xenon scintillation detectors (e.g. Xenon100, LUX)

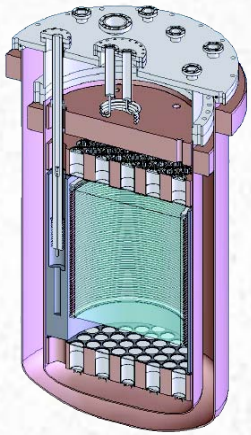

Directionally sensitive (e.g. DRIFT, DMTPC)

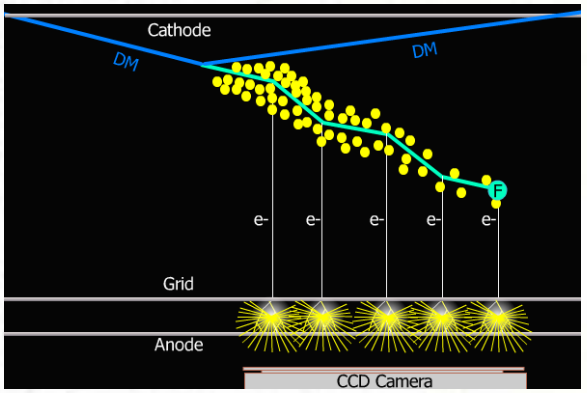

$$\frac{dR}{dE_R} = N_T M_N \frac{\rho_\chi \sigma_n}{2 m_\chi \mu_{ne}^2} \frac{(f_p Z + f_n (A-Z))^2}{f_n^2} F^2[E_R] \int_{\beta_{min}}^{\infty} \frac{f(v)}{v} dv$$

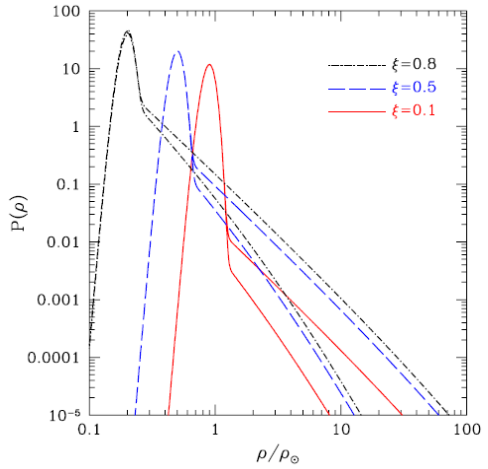

Kamionkowski & Koushiappas (2008)

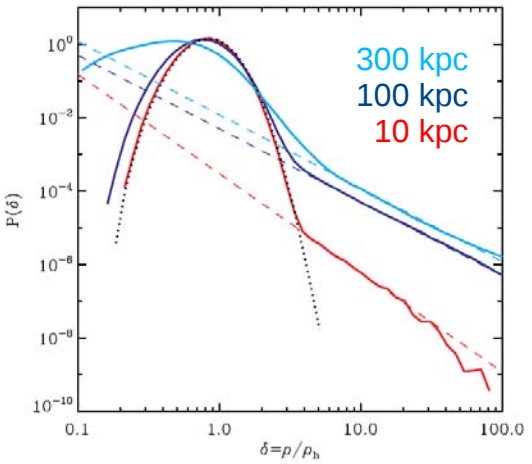

Kamionkowski, Koushiappas & MK (2010)
(see also Vogelsberger et al. 2009)

4) Substructure And Direct Detection

Cryogenic phonon detection (e.g. CDMS)

Liquid Xenon scintillation detectors (e.g. Xenon100, LUX)

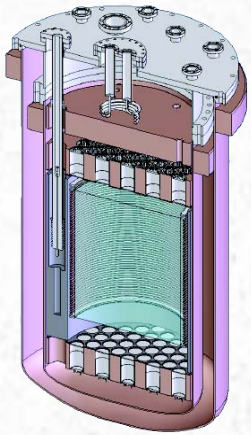

Directionally sensitive (e.g. DRIFT, DMTPC)

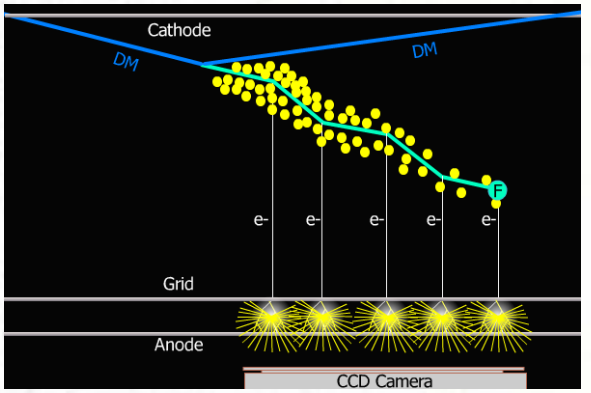

$$\frac{dR}{dE_R} = N_T M_N \frac{\rho_\chi \sigma_n}{2 m_\chi \mu_{ne}^2} \frac{(f_p Z + f_n (A - Z))^2}{f_n^2} F^2[E_R] \int_{\beta_{min}}^{\infty} \frac{f(v)}{v} dv$$

Velocity Space Substructure

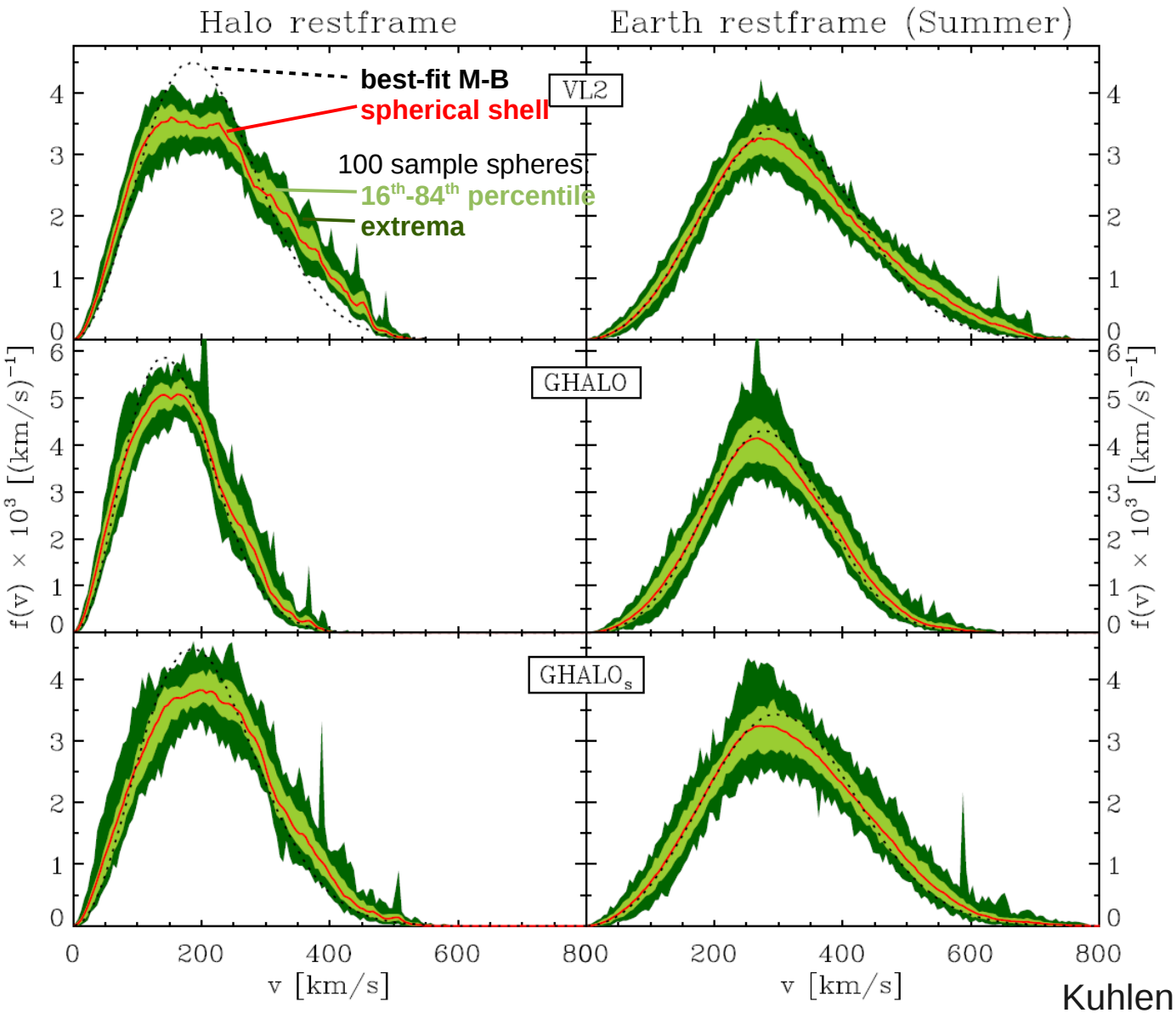

Kuhlen et al. (2010)

See also: Hansen et al. (2005), Vogelsberger et al. (2009)

4) Substructure And Direct Detection

Cryogenic phonon detection (e.g. CDMS)

Liquid Xenon scintillation detectors (e.g. Xenon100, LUX)

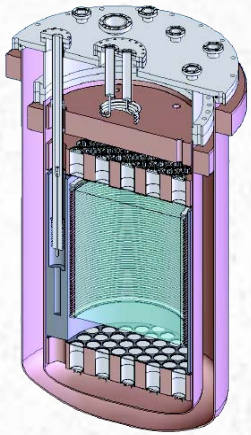

Directionally sensitive (e.g. DRIFT, DMTPC)

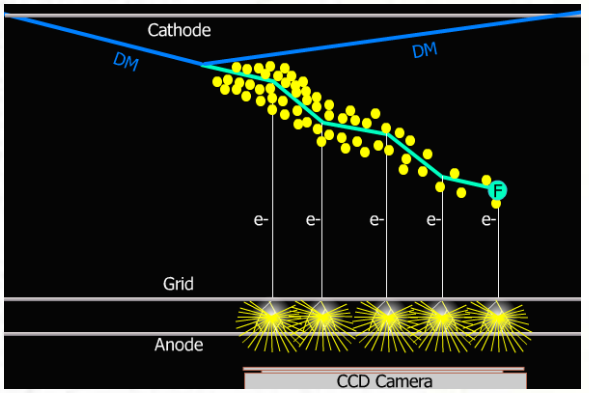

$$\frac{dR}{dE_R} = N_T M_N \frac{\rho_\chi \sigma_n}{2 m_\chi \mu_{ne}^2} \frac{(f_p Z + f_n (A-Z))^2}{f_n^2} F^2[E_R] \int_{\beta_{min}}^{\infty} \frac{f(v)}{v} dv$$

$$\beta_{\min} = \sqrt{\frac{1}{2 m_N E_R}} \left(\frac{m_N E_R}{\mu} + \delta \right)$$

f(v) is not Maxwellian!

Substructures can be important if β_{min} is large.

- Inelastic DM (δ>0)
- Light DM (M_χ<10GeV)
- Directionally sensitive experiments often require high E_{recoil}, large β_{min}.

4) Substructure And Direct Detection

Tables of $g(v_{\rm min}) = \int_{v_{\rm min}}^{\infty} \frac{f(v)}{v}\, dv$ are available for download, at:

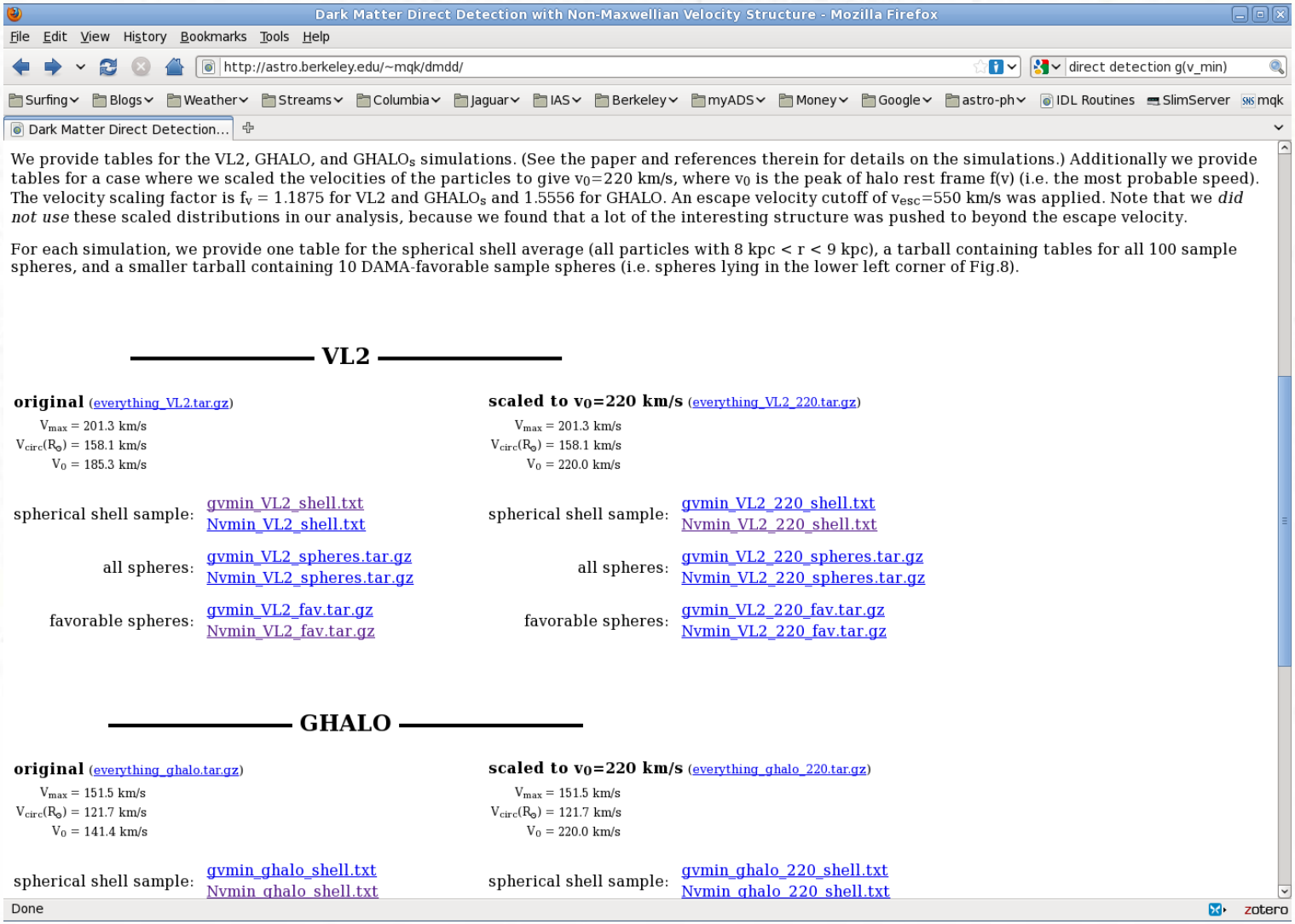

Dark Matter Direct Detection with Non-Maxwellian Velocity Structure - Mozilla Firefox

File Edit View History Bookmarks Tools Help

http://astro.berkeley.edu/~mqk/dmdd/

direct detection g(v_min)

Surfing Blogs Weather Streams Columbia Jaguar IAS Berkeley myADS Money Google astro-ph IDL Routines SlimServer mqk

Dark Matter Direct Detection...

We provide tables for the VL2, GHALO, and GHALO$_s$ simulations. (See the paper and references therein for details on the simulations.) Additionally we provide tables for a case where we scaled the velocities of the particles to give v_0=220 km/s, where v_0 is the peak of halo rest frame f(v) (i.e. the most probable speed). The velocity scaling factor is f_v = 1.1875 for VL2 and GHALO$_s$ and 1.5556 for GHALO. An escape velocity cutoff of v_{esc}=550 km/s was applied. Note that we *did not use* these scaled distributions in our analysis, because we found that a lot of the interesting structure was pushed to beyond the escape velocity.

For each simulation, we provide one table for the spherical shell average (all particles with 8 kpc < r < 9 kpc), a tarball containing tables for all 100 sample spheres, and a smaller tarball containing 10 DAMA-favorable sample spheres (i.e. spheres lying in the lower left corner of Fig.8).

VL2

original (everything_VL2.tar.gz)

V_{max} = 201.3 km/s
$V_{circ}(R_\odot)$ = 158.1 km/s
V_0 = 185.3 km/s

spherical shell sample:	gvmin_VL2_shell.txt Nvmin_VL2_shell.txt
all spheres:	gvmin_VL2_spheres.tar.gz Nvmin_VL2_spheres.tar.gz
favorable spheres:	gvmin_VL2_fav.tar.gz Nvmin_VL2_fav.tar.gz

scaled to v_0=220 km/s (everything_VL2_220.tar.gz)

V_{max} = 201.3 km/s
$V_{circ}(R_\odot)$ = 158.1 km/s
V_0 = 220.0 km/s

spherical shell sample:	gvmin_VL2_220_shell.txt Nvmin_VL2_220_shell.txt
all spheres:	gvmin_VL2_220_spheres.tar.gz Nvmin_VL2_220_spheres.tar.gz
favorable spheres:	gvmin_VL2_220_fav.tar.gz Nvmin_VL2_220_fav.tar.gz

GHALO

original (everything_ghalo.tar.gz)

V_{max} = 151.5 km/s
$V_{circ}(R_\odot)$ = 121.7 km/s
V_0 = 141.4 km/s

spherical shell sample:	gvmin_ghalo_shell.txt Nvmin_ghalo_shell.txt

scaled to v_0=220 km/s (everything_ghalo_220.tar.gz)

V_{max} = 151.5 km/s
$V_{circ}(R_\odot)$ = 121.7 km/s
V_0 = 220.0 km/s

spherical shell sample:	gvmin_ghalo_220_shell.txt Nvmin_ghalo_220_shell.txt

Done

zotero

4) Substructure And Direct Detection

Tables of $g(v_{\rm min}) = \int_{v_{\rm min}}^{\infty} \frac{f(v)}{v}\, dv$ are available for download, at:

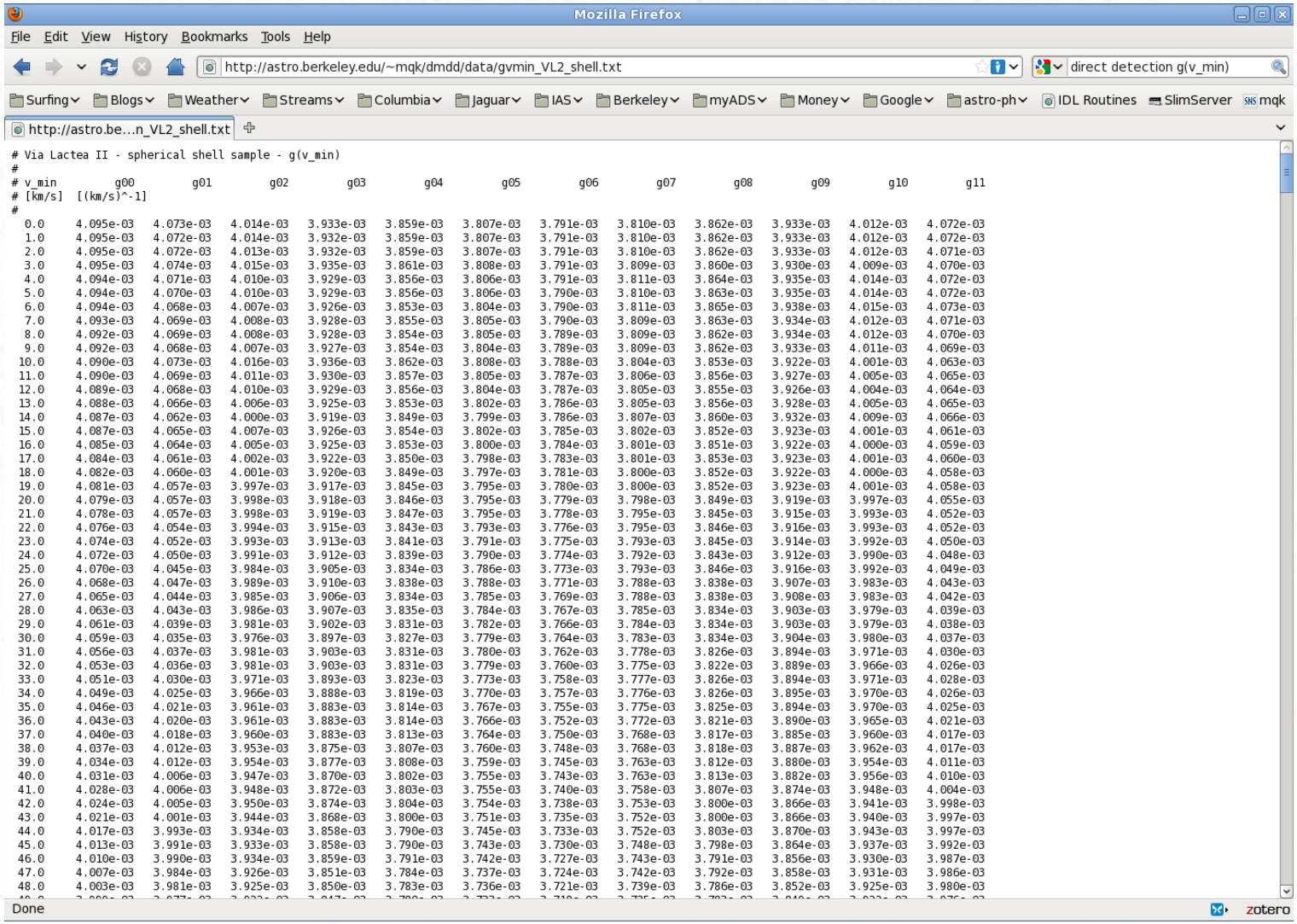


```
# Via Lactea II - spherical shell sample - g(v_min)
#
# v_min        g00         g01         g02         g03         g04         g05         g06         g07         g08         g09         g10         g11
# [km/s]  [(km/s)^-1]
#
  0.0     4.095e-03   4.073e-03   4.014e-03   3.933e-03   3.859e-03   3.807e-03   3.791e-03   3.810e-03   3.862e-03   3.933e-03   4.012e-03   4.072e-03
  1.0     4.095e-03   4.072e-03   4.014e-03   3.932e-03   3.859e-03   3.807e-03   3.791e-03   3.810e-03   3.862e-03   3.933e-03   4.012e-03   4.072e-03
  2.0     4.095e-03   4.072e-03   4.013e-03   3.932e-03   3.859e-03   3.807e-03   3.791e-03   3.810e-03   3.862e-03   3.933e-03   4.012e-03   4.071e-03
  3.0     4.095e-03   4.074e-03   4.015e-03   3.935e-03   3.861e-03   3.808e-03   3.791e-03   3.809e-03   3.860e-03   3.930e-03   4.009e-03   4.070e-03
  4.0     4.094e-03   4.071e-03   4.010e-03   3.929e-03   3.856e-03   3.806e-03   3.791e-03   3.811e-03   3.864e-03   3.935e-03   4.014e-03   4.072e-03
  5.0     4.094e-03   4.070e-03   4.010e-03   3.929e-03   3.856e-03   3.806e-03   3.790e-03   3.810e-03   3.863e-03   3.935e-03   4.014e-03   4.072e-03
  6.0     4.094e-03   4.068e-03   4.007e-03   3.926e-03   3.853e-03   3.804e-03   3.790e-03   3.811e-03   3.865e-03   3.938e-03   4.015e-03   4.073e-03
  7.0     4.093e-03   4.069e-03   4.008e-03   3.928e-03   3.855e-03   3.805e-03   3.790e-03   3.809e-03   3.863e-03   3.934e-03   4.012e-03   4.071e-03
  8.0     4.092e-03   4.069e-03   4.008e-03   3.928e-03   3.854e-03   3.805e-03   3.789e-03   3.809e-03   3.862e-03   3.934e-03   4.012e-03   4.070e-03
  9.0     4.092e-03   4.068e-03   4.007e-03   3.927e-03   3.854e-03   3.804e-03   3.789e-03   3.809e-03   3.862e-03   3.933e-03   4.011e-03   4.069e-03
 10.0     4.090e-03   4.073e-03   4.016e-03   3.936e-03   3.862e-03   3.808e-03   3.788e-03   3.804e-03   3.853e-03   3.922e-03   4.001e-03   4.063e-03
 11.0     4.090e-03   4.069e-03   4.011e-03   3.930e-03   3.857e-03   3.805e-03   3.787e-03   3.806e-03   3.856e-03   3.927e-03   4.005e-03   4.065e-03
 12.0     4.089e-03   4.068e-03   4.010e-03   3.929e-03   3.856e-03   3.804e-03   3.787e-03   3.805e-03   3.855e-03   3.926e-03   4.004e-03   4.064e-03
 13.0     4.088e-03   4.066e-03   4.006e-03   3.925e-03   3.853e-03   3.802e-03   3.786e-03   3.805e-03   3.856e-03   3.928e-03   4.005e-03   4.065e-03
 14.0     4.087e-03   4.062e-03   4.000e-03   3.919e-03   3.849e-03   3.799e-03   3.786e-03   3.807e-03   3.860e-03   3.932e-03   4.009e-03   4.066e-03
 15.0     4.087e-03   4.065e-03   4.007e-03   3.926e-03   3.854e-03   3.802e-03   3.785e-03   3.802e-03   3.852e-03   3.923e-03   4.001e-03   4.061e-03
 16.0     4.085e-03   4.064e-03   4.005e-03   3.925e-03   3.853e-03   3.800e-03   3.784e-03   3.801e-03   3.851e-03   3.922e-03   4.000e-03   4.059e-03
 17.0     4.084e-03   4.061e-03   4.002e-03   3.922e-03   3.850e-03   3.798e-03   3.783e-03   3.801e-03   3.853e-03   3.923e-03   4.001e-03   4.060e-03
 18.0     4.082e-03   4.060e-03   4.001e-03   3.920e-03   3.849e-03   3.797e-03   3.781e-03   3.800e-03   3.852e-03   3.922e-03   4.000e-03   4.058e-03
 19.0     4.081e-03   4.057e-03   3.997e-03   3.917e-03   3.845e-03   3.795e-03   3.780e-03   3.800e-03   3.852e-03   3.923e-03   4.001e-03   4.058e-03
 20.0     4.079e-03   4.057e-03   3.998e-03   3.918e-03   3.846e-03   3.795e-03   3.779e-03   3.798e-03   3.849e-03   3.919e-03   3.997e-03   4.055e-03
 21.0     4.078e-03   4.057e-03   3.998e-03   3.919e-03   3.847e-03   3.795e-03   3.778e-03   3.795e-03   3.845e-03   3.915e-03   3.993e-03   4.052e-03
 22.0     4.076e-03   4.054e-03   3.994e-03   3.915e-03   3.843e-03   3.793e-03   3.776e-03   3.795e-03   3.846e-03   3.916e-03   3.993e-03   4.052e-03
 23.0     4.074e-03   4.052e-03   3.993e-03   3.913e-03   3.841e-03   3.791e-03   3.775e-03   3.793e-03   3.845e-03   3.914e-03   3.992e-03   4.050e-03
 24.0     4.072e-03   4.050e-03   3.991e-03   3.912e-03   3.839e-03   3.790e-03   3.774e-03   3.792e-03   3.843e-03   3.912e-03   3.990e-03   4.048e-03
 25.0     4.070e-03   4.045e-03   3.984e-03   3.905e-03   3.834e-03   3.786e-03   3.773e-03   3.793e-03   3.846e-03   3.916e-03   3.992e-03   4.049e-03
 26.0     4.068e-03   4.047e-03   3.989e-03   3.910e-03   3.838e-03   3.788e-03   3.771e-03   3.788e-03   3.838e-03   3.907e-03   3.983e-03   4.043e-03
 27.0     4.065e-03   4.044e-03   3.985e-03   3.906e-03   3.834e-03   3.785e-03   3.769e-03   3.788e-03   3.838e-03   3.908e-03   3.983e-03   4.042e-03
 28.0     4.063e-03   4.043e-03   3.986e-03   3.907e-03   3.835e-03   3.784e-03   3.767e-03   3.785e-03   3.834e-03   3.903e-03   3.979e-03   4.039e-03
 29.0     4.061e-03   4.039e-03   3.981e-03   3.902e-03   3.831e-03   3.782e-03   3.766e-03   3.784e-03   3.834e-03   3.903e-03   3.979e-03   4.038e-03
 30.0     4.059e-03   4.035e-03   3.976e-03   3.897e-03   3.827e-03   3.779e-03   3.764e-03   3.783e-03   3.834e-03   3.904e-03   3.980e-03   4.037e-03
 31.0     4.056e-03   4.037e-03   3.981e-03   3.903e-03   3.831e-03   3.780e-03   3.762e-03   3.778e-03   3.826e-03   3.894e-03   3.971e-03   4.030e-03
 32.0     4.053e-03   4.036e-03   3.981e-03   3.903e-03   3.831e-03   3.779e-03   3.760e-03   3.775e-03   3.822e-03   3.889e-03   3.966e-03   4.026e-03
 33.0     4.051e-03   4.030e-03   3.971e-03   3.893e-03   3.823e-03   3.773e-03   3.758e-03   3.777e-03   3.826e-03   3.894e-03   3.971e-03   4.028e-03
 34.0     4.049e-03   4.025e-03   3.966e-03   3.888e-03   3.819e-03   3.770e-03   3.757e-03   3.776e-03   3.826e-03   3.895e-03   3.970e-03   4.026e-03
 35.0     4.046e-03   4.021e-03   3.961e-03   3.883e-03   3.814e-03   3.767e-03   3.755e-03   3.775e-03   3.825e-03   3.894e-03   3.970e-03   4.025e-03
 36.0     4.043e-03   4.020e-03   3.961e-03   3.883e-03   3.814e-03   3.766e-03   3.752e-03   3.772e-03   3.821e-03   3.890e-03   3.965e-03   4.021e-03
 37.0     4.040e-03   4.018e-03   3.960e-03   3.883e-03   3.813e-03   3.764e-03   3.750e-03   3.768e-03   3.817e-03   3.885e-03   3.960e-03   4.017e-03
 38.0     4.037e-03   4.012e-03   3.953e-03   3.875e-03   3.807e-03   3.760e-03   3.748e-03   3.768e-03   3.818e-03   3.887e-03   3.962e-03   4.017e-03
 39.0     4.034e-03   4.012e-03   3.954e-03   3.877e-03   3.808e-03   3.759e-03   3.745e-03   3.763e-03   3.812e-03   3.880e-03   3.954e-03   4.011e-03
 40.0     4.031e-03   4.006e-03   3.947e-03   3.870e-03   3.802e-03   3.755e-03   3.743e-03   3.763e-03   3.813e-03   3.882e-03   3.956e-03   4.010e-03
 41.0     4.028e-03   4.006e-03   3.948e-03   3.872e-03   3.803e-03   3.755e-03   3.740e-03   3.758e-03   3.807e-03   3.874e-03   3.948e-03   4.004e-03
 42.0     4.024e-03   4.005e-03   3.950e-03   3.874e-03   3.804e-03   3.754e-03   3.738e-03   3.753e-03   3.800e-03   3.866e-03   3.941e-03   3.998e-03
 43.0     4.021e-03   4.001e-03   3.944e-03   3.868e-03   3.800e-03   3.751e-03   3.735e-03   3.752e-03   3.800e-03   3.866e-03   3.940e-03   3.997e-03
 44.0     4.017e-03   3.993e-03   3.934e-03   3.858e-03   3.790e-03   3.745e-03   3.733e-03   3.752e-03   3.803e-03   3.870e-03   3.943e-03   3.997e-03
 45.0     4.013e-03   3.991e-03   3.933e-03   3.858e-03   3.790e-03   3.743e-03   3.730e-03   3.748e-03   3.798e-03   3.864e-03   3.937e-03   3.992e-03
 46.0     4.010e-03   3.990e-03   3.934e-03   3.859e-03   3.791e-03   3.742e-03   3.727e-03   3.743e-03   3.791e-03   3.856e-03   3.930e-03   3.987e-03
 47.0     4.007e-03   3.984e-03   3.926e-03   3.851e-03   3.784e-03   3.737e-03   3.724e-03   3.742e-03   3.792e-03   3.858e-03   3.931e-03   3.986e-03
 48.0     4.003e-03   3.981e-03   3.925e-03   3.850e-03   3.783e-03   3.736e-03   3.721e-03   3.739e-03   3.786e-03   3.852e-03   3.925e-03   3.980e-03
```

4) Substructure And Direct Detection

McCabe (2010) made use of these tables to evaluate the dependence of exclusion limits from CDMS-II(Si), CDMS-II(Ge), CRESST-II, XENON10 on the f(v) variation from the VL2/GHALO simulations.

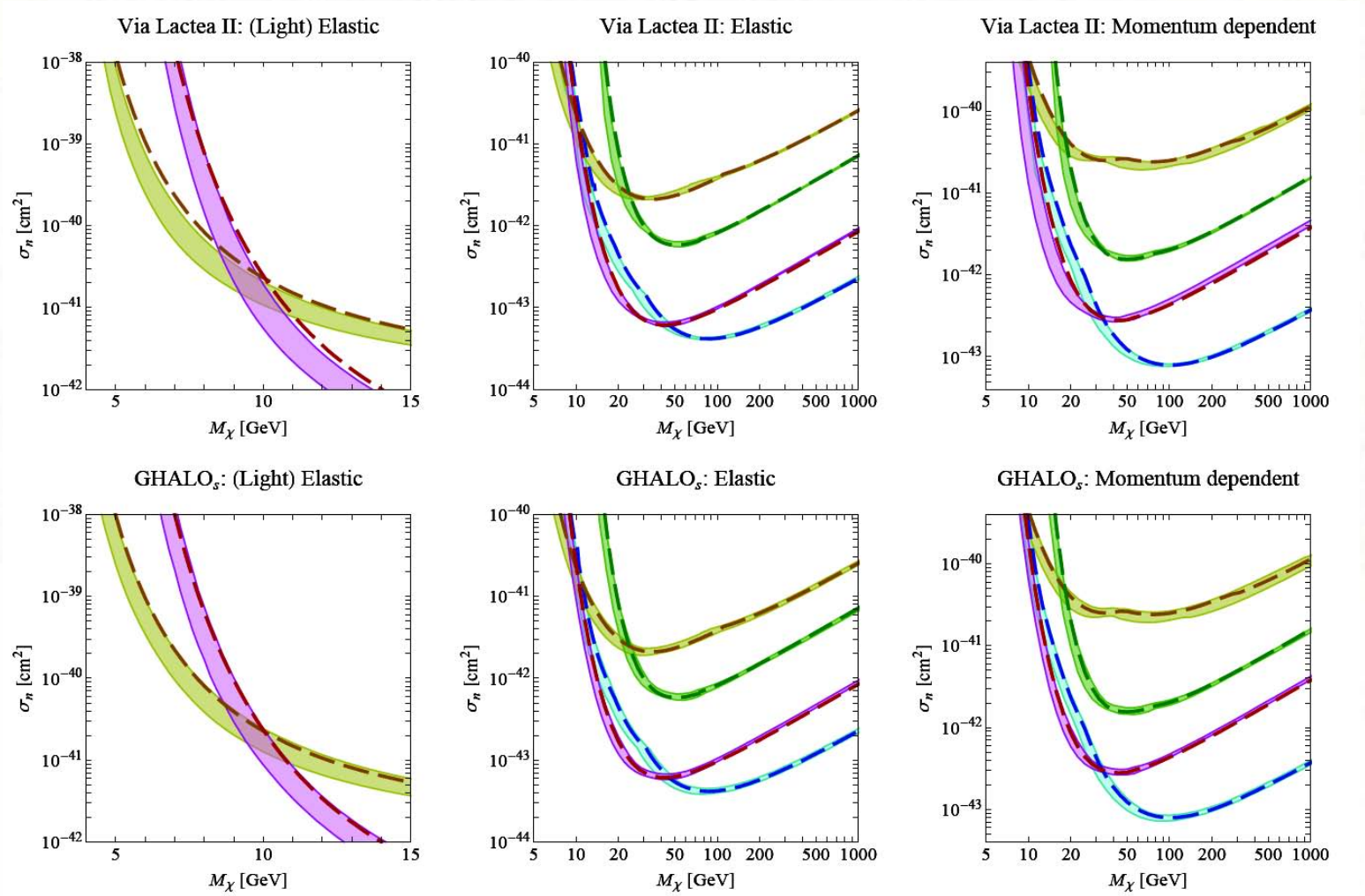

Velocity Direction in **Halo Rest Frame**

Maxwell-Boltzmann (isotropic)

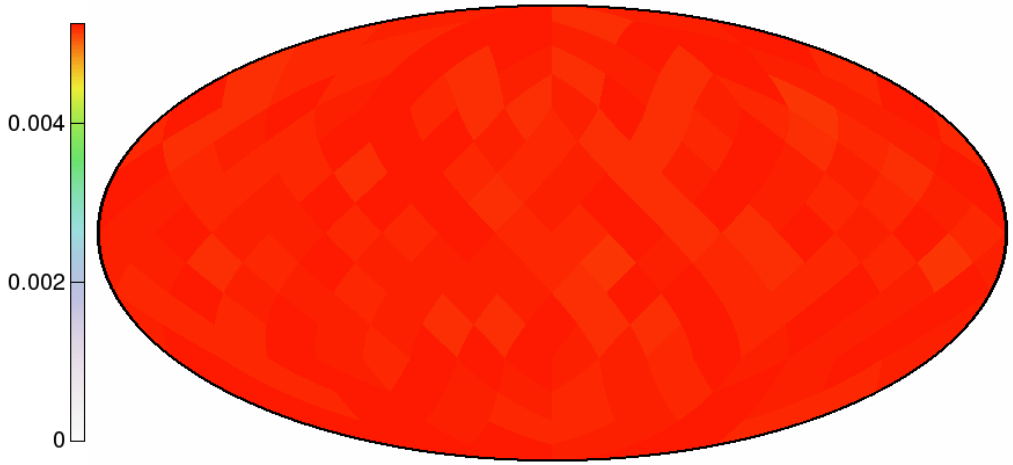

Spherical Shell (8 kpc < R < 9 kpc)

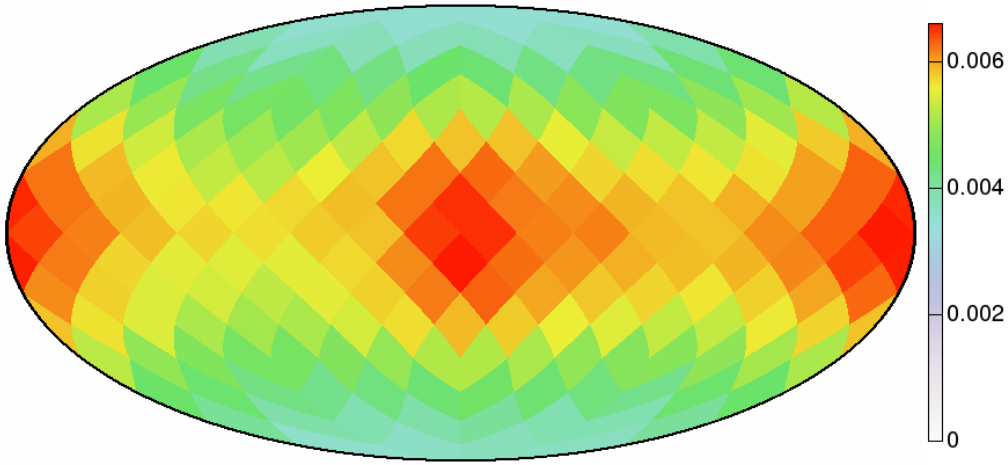

Sample Sphere #001

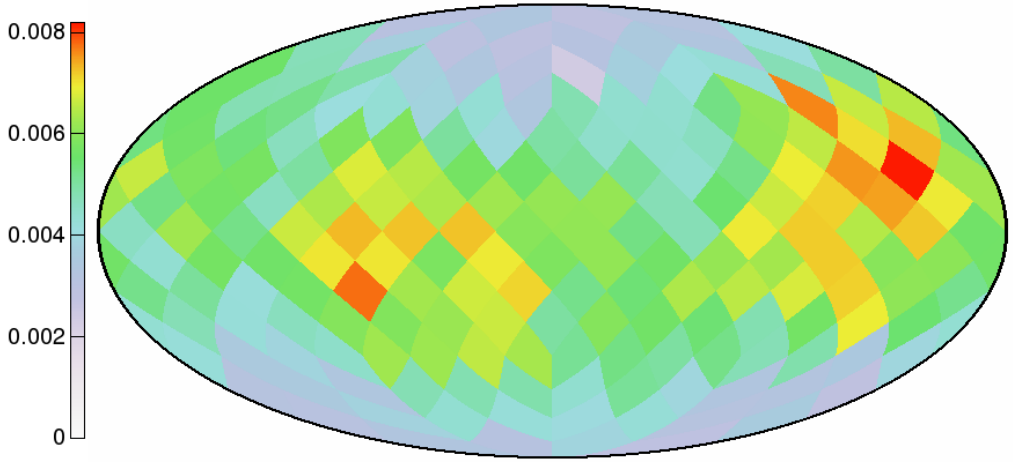

Sample Sphere #004 (containing a subhalo)

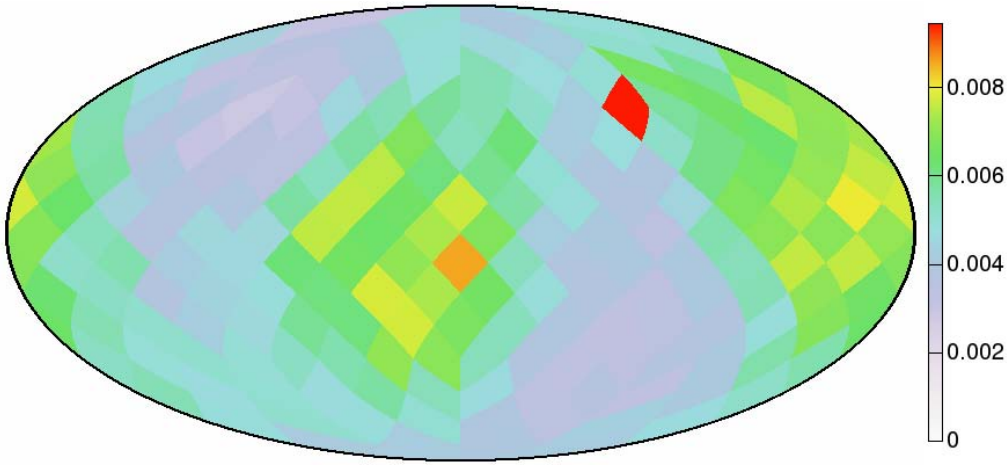

… in **Earth Rest Frame v_{min}= 0 km/s**

Maxwell-Boltzmann (isotropic)

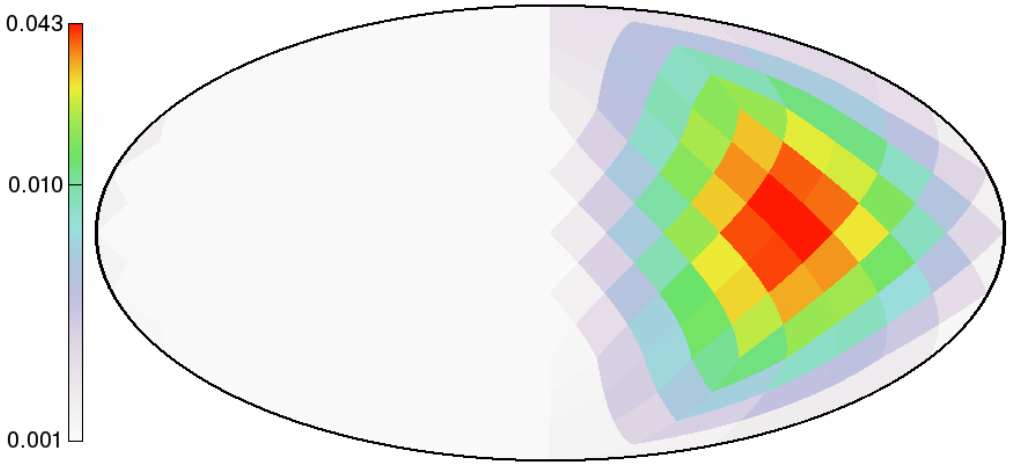

Spherical Shell (8 kpc < R < 9 kpc)

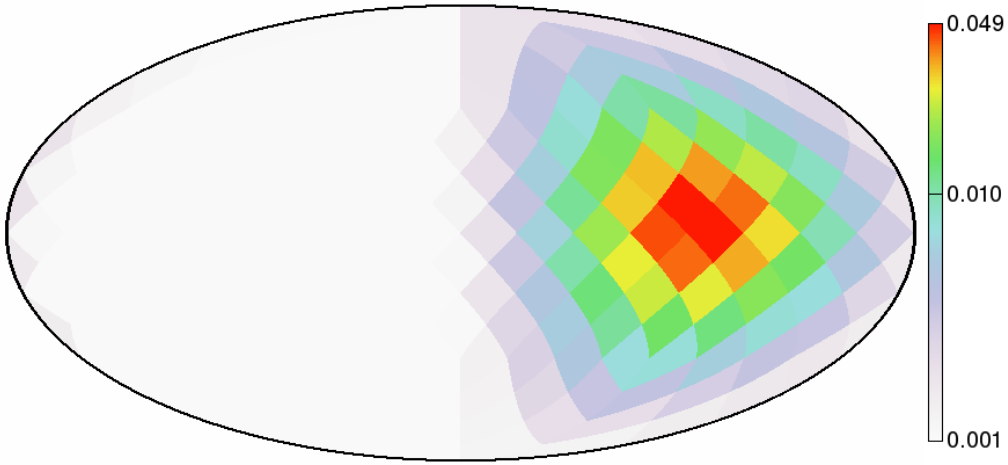

Sample Sphere #001

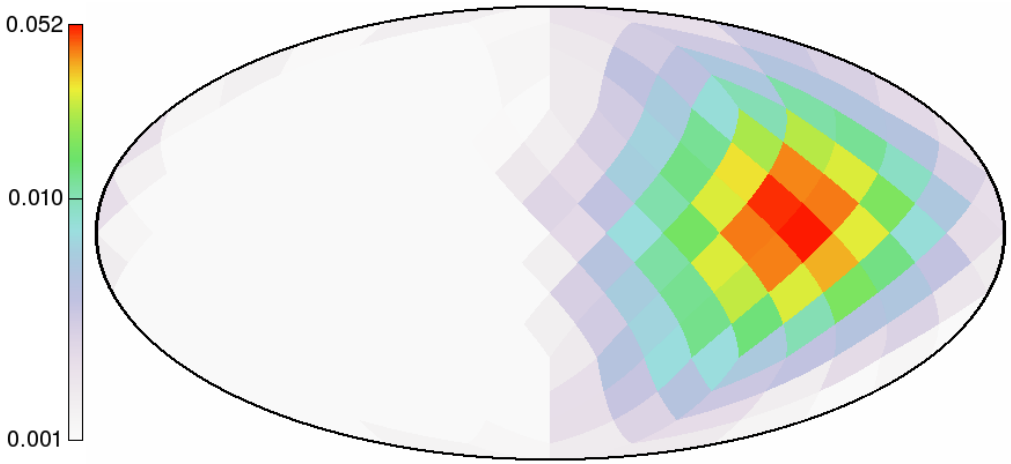

Sample Sphere #004 (containing a subhalo)

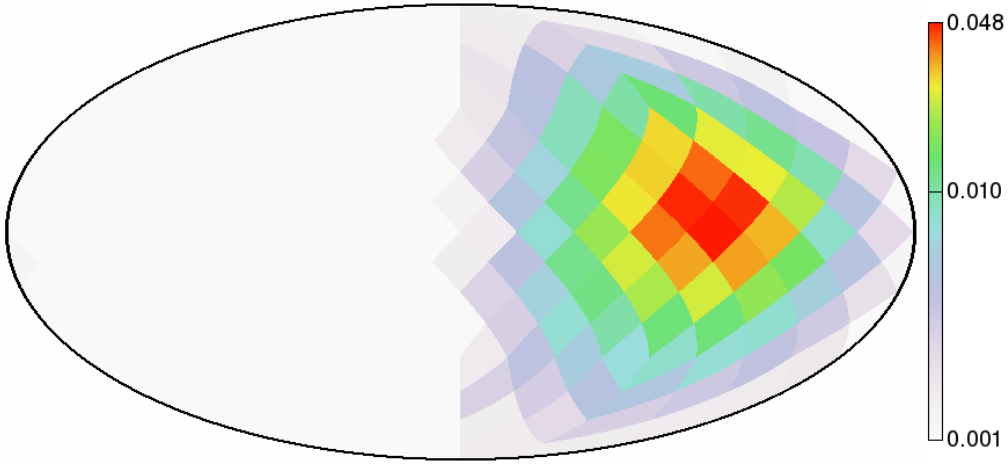

… in **Earth Rest Frame v_{min}= 500 km/s**

Maxwell-Boltzmann (isotropic)

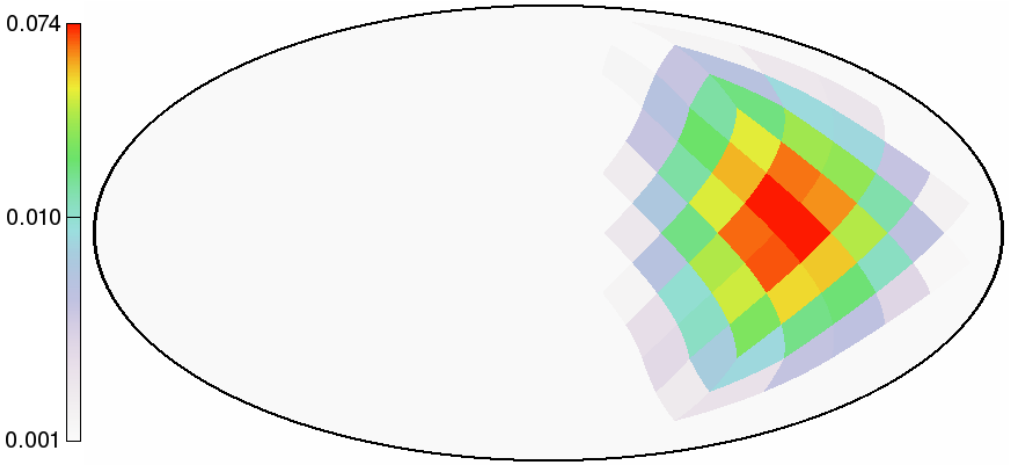

Spherical Shell (8 kpc < R < 9 kpc)

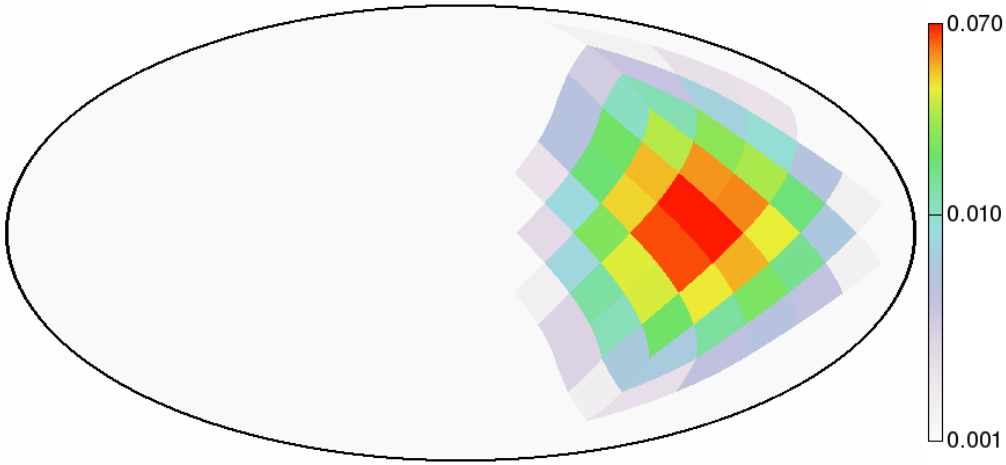

Sample Sphere #001

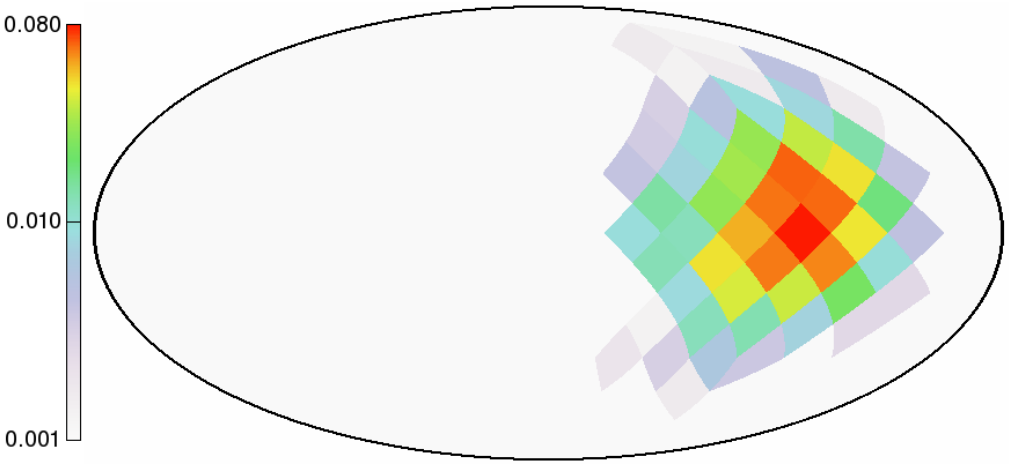

Sample Sphere #004 (containing a subhalo)

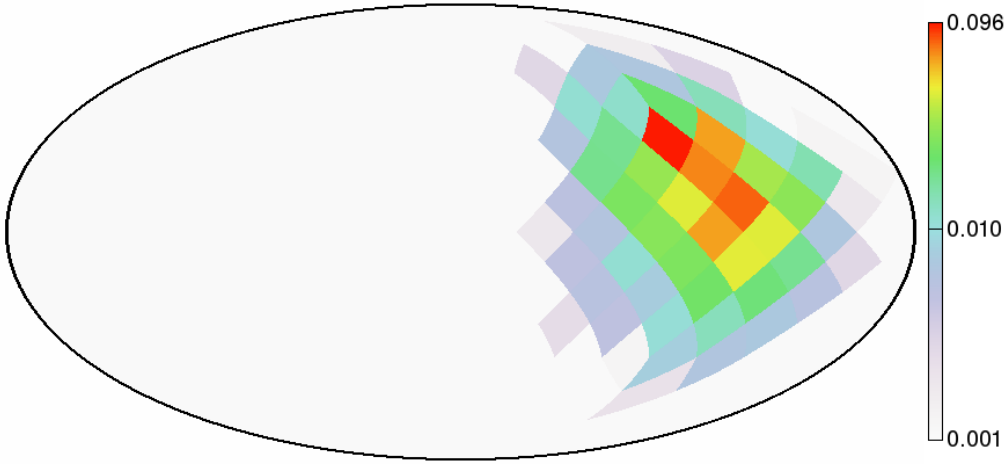

… in **Earth Rest Frame v_{min}= 500 km/s**

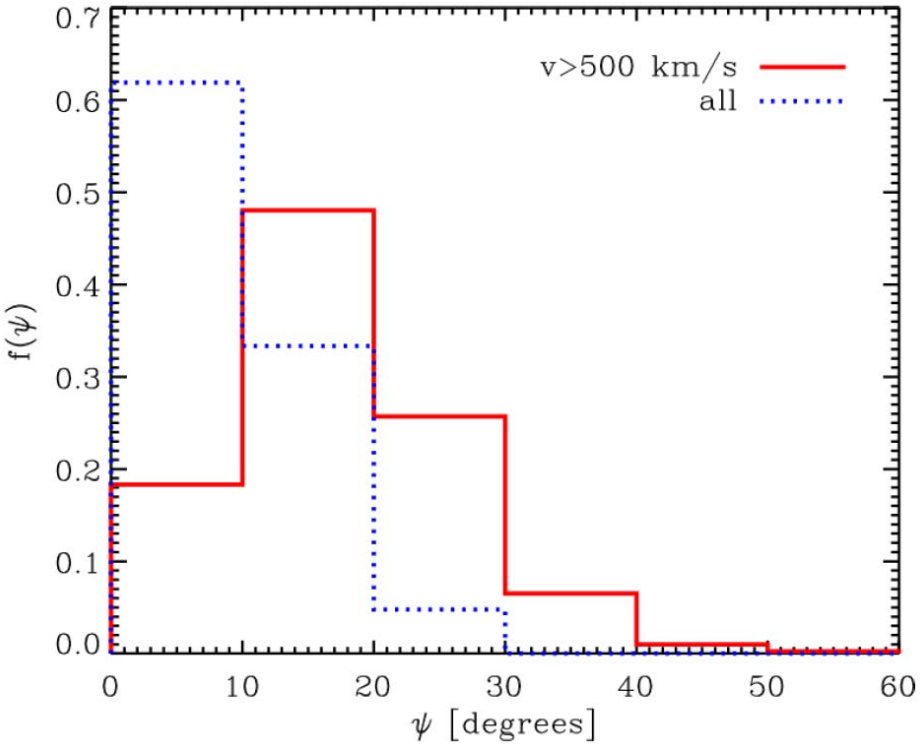

Sample Sphere #004 (containing a subhalo)

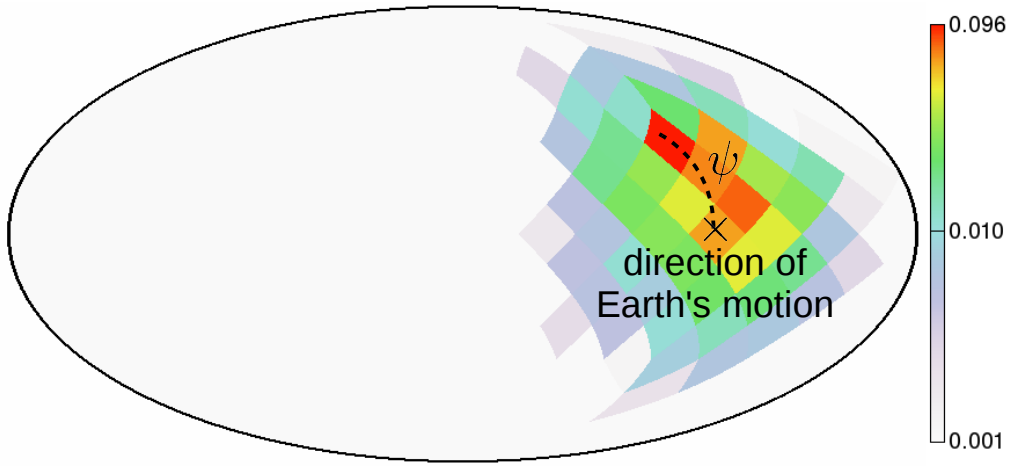

At v_{min}=500 km/s the hotspot is more than 10° away from the direction of Earth's motion in ~80% of all cases!

Conclusions

- The number of subhalos resolved in the to-date largest simulations (Via Lactea II, GHALO, Aquarius) is ever increasing: >300,000 at latest count. Also lots of velocity substructure from subhalos and tidal streams.
- Once properly scaled, the Via Lactea, GHALO, and Aquarius simulations give consistent results.
- Simulations predict that Fermi should discover a handful of subhalos over its lifetime if the DM mass is <100 GeV and it annihilates through $b\bar{b}$. So far only limits.
- The annihilation boost factor from substructure depends on radius: at the GC or at the Sun it's not likely to be important.
- The total luminosity boost factor critically depends on the extrapolation of the subhalo concentration-mass relation.
- Velocity substructure in the DM distribution function might noticeably affect DM direct detection experiments, especially for DM models or experimental setups that are sensitive to high velocity DM particles: e.g. inelastic DM, light DM, directionally sensitive experiments.